https://doi.org/10.5194/egusphere-2026-5997
Preprint. Discussion started: 20 October 2026
© Author(s) 2026. CC BY 4.0 License.

Assessment of year-round snow depth on Arctic sea ice

Anne Braakmann-Folgmann[1], Jack C. Landy[1], Stefan Hendricks[2], Clara Vydra[1,3], Robert Ricker[4], and Alessandro Di Bella[5]

[1]UiT The Arctic University of Norway, 9019 Tromsø, Norway
[2]Alfred Wegener Institute, Helmholtz Centre for Polar and Marine Research, Bremerhaven, Germany
[3]European Commission Joint Research Centre, Ispra, Italy
[4]NORCE Norwegian Research Centre, 9019 Tromsø, Norway
[5]European Space Agency, Via Galileo Galilei 2, 00044 Frascati, Italy

Correspondence: Anne Braakmann-Folgmann (anne.bf@uit.no)

Abstract. Snow on sea ice is an essential climate variable due to its high albedo and insulating capability. In addition, snow thickness estimates are needed to calculate sea ice freeboard and thickness (SIT) from radar altimetry measurements and uncertainties in snow depth contribute significantly to the resulting SIT uncertainty. In recent years, progress has been made observing or estimating winter snow depth. However, very few snow depth products exist year-round, i.e. including the summer melt season, despite considerable snow remaining on the ice in early summer. This study is the first to assess snow depth estimates year-round with a focus on the so far unexplored melt season. We intercompare estimates (a) based on in situ data from the Warren climatology and (b) two modified Warren climatologies using either ice age data or ice charts, (c) modeled snow depth from SnowModel-LG using two different forcings, (d) a climatology of SnowModel-LG, (e) a combination of the modified Warren climatology and the SnowModel-LG climatology, and (f) finally we also, for the first time, explore the use of dual-frequency altimetry (KuLa) to derive snow depth estimates year-round. We compare the snow depth products against buoy observations of snow depth and airborne measurements of SIT, as well as mooring measurements of sea ice draft together with CryoSat-2 freeboard data. We find that the MERRA-2 forced version of SnowModel-LG agrees better with validation data during the melt season, because the ERA-5 forced version melts the snow much faster than any other product. When a Warren climatology is used, we recommend using the modified version and to strictly only use it in the Central Arctic, where it is constrained by measurements. For KuLa we find that realistic results extend into summer. However, some regions retain snow throughout summer, which likely indicates residual negative biases in CryoSat-2 freeboards and/or positive biases in the ICESat-2 freeboard data.

1 Introduction

Snow on sea ice plays a critical role in the Arctic climate system due to its high albedo, contribution to the Arctic freshwater budget, and influence on energy exchange processes. During the spring and summer months, snow depth determines the availability of light under the sea ice, impacting primary productivity (Kauko et al., 2017), and acts as essential denning habitat for seals and polar bears (Hamilton et al., 2017). In addition, information on the snow mass is required when converting the observed radar freeboard to sea ice freeboard and to estimate sea ice thickness (SIT, Zygmuntowska et al. (2014)). While most

https://doi.org/10.5194/egusphere-2026-5997
Preprint. Discussion started: 20 October 2026
© Author(s) 2026. CC BY 4.0 License.

of the snow cover melts during summer, considerable snow remains on the ice in early summer and some snow accumulation happens throughout the summer months (Chapman-Dutton and Webster, 2024). Hence, we need a good estimate of snow depth also during the summer months in order to derive SIT year-round.

Concerning SIT, recent developments have enabled the first year-round sea ice thickness products from CryoSat-2 (Landy et al., 2022) and ICESat-2 (Petty et al., 2025a). While the CryoSat-2 estimates use a summer-specific classification algorithm to differentiate leads from melt pond covered sea ice (Dawson et al., 2022; Braakmann-Folgmann et al., 2026), misclassification of melt ponds as leads from ICESat-2 is mitigated by filtering later on (Petty et al., 2025a). The resulting SIT shows decent agreement between the two sensors as well as with validation data (Landy et al., 2022; Petty et al., 2025a; Buckley et al., 2026). In general, summer estimates are more uncertain than during the winter months, but the novel products have proven to add skill to sea ice forecasts (Song et al., 2024; Zhang et al., 2023). A key remaining uncertainty for year-round SIT is the snow depth on sea ice during the summer months (Petty et al., 2025a) and the fact that very few products are available-year round.

A range of methods have been developed to estimate snow depth on Arctic sea ice using in situ observations (Warren et al., 1999; Shalina and Sandven, 2018), passive microwave data (Comiso et al., 2003; Rostosky et al., 2018; Braakmann-Folgmann and Donlon, 2019), dual-frequency altimetry (Guerreiro et al., 2016; Lawrence et al., 2018; Kacimi and Kwok, 2022; Carret et al., 2025) and models (Liston et al., 2020; Zhang and Rothrock, 2003). However, most of these methods struggle in the melt season, when wet snow becomes a black body to passive microwave sensors (Markus et al., 2006) and altimeters cannot easily differentiate between melt ponds and leads (Braakmann-Folgmann et al., 2026) or can be impacted by shifts in the dominant height of radar backscattering (Taelman et al., 2026). Hence, most snow depth products are limited to the cold season (October - April) and both method development and a previous intercomparison study have focused on this period (Zhou et al., 2021). The upcoming ESA CRISTAL (Copernicus Polar Ice and Snow Topography Altimeter) mission is expected to deliver snow on sea ice measurements from the difference of Ka- and Ku-Band freeboards along the same ground track, i.e. collocated with freeboard measurements. However, also here the applicability to the melt season remains uncertain. Currently, snow depth retrievals from a combination of CryoSat-2 Ku-band and SARAL/AltiKa Ka-band are limited to the winter months (Guerreiro et al., 2016; Lawrence et al., 2018), but partly because the Arctic sea ice cover retreats to mostly within the SARAL/Altika pole hole during summer. This is the first study to assess snow depth products year-round and with a focus on the summer months, for which almost no validation has so far been conducted.

The few existing snow depth estimates that cover the summer months are the original and modified Warren climatologies and SnowModel-LG. As the latter is not updated operationally, we also build a climatology from 13 years of data and compare the results to estimates from the specific years (where available). We also test a combination of Warren and SnowModel-LG, as introduced in the baseline-E winter and summer sea ice ESA CryoTEMPO (CryoSat ThEMatic PrOducts) products (European Space Agency, 2026). In addition, we calculate and assess the ICESat-2 versus CryoSat-2 dual-altimetry difference (KuLa) year round to test its applicability for the summer months. KuLa yields good results in winter (Carret et al., 2025), but has so far never been applied year-round. With the recent advances in CryoSat-2 and ICESat-2 freeboard estimates over the summer season, we now test its applicability in summer too.

https://doi.org/10.5194/egusphere-2026-5997
Preprint. Discussion started: 20 October 2026
© Author(s) 2026. CC BY 4.0 License.

2 Snow depth products

This section introduces the various snow depth products assessed in this paper. Table 1 gives an overview of the spatial and temporal sampling and coverage of all input data.

2.1 (Modified) Warren climatology - W99, mW99-IA, mW99-IC

The Warren climatology (W99) was developed by Warren et al. (1999) based on in-situ measurements from Soviet drifting stations between 1954-1991, primarily over multiyear ice (MYI) and in the Central Arctic. Owing to a lack of suitable operational alternatives, this climatology is still the basis for regularly used snow depth parametrisations. It has conventionally been applied to the winter months and is yet to be tested for summer months, but the climatology itself is year-round. W99 is defined by a polynomial function of 2nd order at monthly intervals. Since it is only constrained by observations in the Central Arctic, we only use it there. Our validation experiments show extremely high errors in the Barents Sea and Fram Strait, where the Warren polynomial functions are evaluated outside their intended domain. Therefore we do not report these results, but acknowledge the limitation for Arctic-wide applications or studies on the marginal ice zone.

To account for thinner snow depths on first year ice, which was less prevalent and undersampled during the time of the W99 data acquisition, a modified Warren climatology has been suggested. Here, the snow depth estimate of the original climatology is halved in areas of first-year ice (FYI, Kurtz and Farrell (2011)). This requires additional data to differentiate between FYI and MYI. We test two different products that are available year-round to assess the impact of the additional input data. The first one is the NSIDC sea ice age data (Tschudi et al., 2019b) covering the years 1984-2024. Corresponding quick-look data exists up to 2025 (Tschudi et al., 2019a). The ice age data is provided at weekly time intervals and on a 12.5 km grid. We refer to the modified Warren climatology using this ice age data as mW99-IA from here on. The second product is based on the US ice charts of thin ice, FYI and MYI concentration, which is operationally available from NSIDC (U.S. National Ice Center, 2020) since 2003. Just like the ice age data, ice charts are provided on a weekly basis, but at 10 km resolution. We refer to the modified Warren climatology using the ice charts as mW99-IC.

While the ice age data yields an integer value per grid cell (ice age in years), the ice chart gives a percentage of MYI concentration. As we compare all products on an 80 km grid, we build our own "MYI concentration" from the ice age data by calculating the percentage of 12.5 km grid cells within the 80 km grid cell that contain ice older than one year. Thus, we can use MYI concentration from either the ice age data or the ice charts to linearly reduce W99 snow depth in areas of FYI. We multiply W99 snow depth with $0.5 \cdot (1 + \text{MYI fraction})$, i.e. areas with 100 % MYI concentration are equal to W99, in areas with 0 % MYI concentration snow depth is halved and in areas with mixed ice types it is graded in between.

2.2 SnowModel-LG (climatology) - SMLG-M2, SMLG-E5, SMLG-M2-Clim

SnowModel-LG is a Lagrangian snow evolution model, forced with reanalysis data from either MERRA-2 or ERA-5 atmospheric reanalysis data and modeling sea ice drift and snow evolution for each parcel (Liston et al., 2020). It includes new snowfall, the redistribution due to wind, compaction, melt, sublimation, and the formation of superimposed ice. The data is

https://doi.org/10.5194/egusphere-2026-5997
Preprint. Discussion started: 20 October 2026
© Author(s) 2026. CC BY 4.0 License.

	spatial sampling	spatial coverage	temporal sampling	temporal coverage
input data				
Warren 99	- (polynomial function)	Central Arctic	monthly	Climatology (1954-1991)
ice age	12.5 km	Arctic-wide	weekly	1984-2024
ice chart	10 km	Arctic-wide	weekly	2003-now
SMLG	25 km	Arctic-wide	daily	1980-2021
CryoSat-2	along-track	Arctic-wide	daily (with gaps)	2010-now
ICESat-2 ATL20	25 km	Arctic-wide	daily (with gaps)	2018-now
intercomparison				
maps	80 km	Arctic-wide	monthly	2019
timeseries	-	Central Arctic	daily	2010-2024

Table 1. Overview of spatial and temporal sampling and coverage of the input data as well as how the intercomparison and validation are performed

available daily at 25 km resolution. Updated versions are released at irregular intervals and the latest official version covers 1 August 1980 to 31 July 2021 (Liston et al., 2021). Validation has mainly focused on the winter (Stroeve et al., 2020). We refer to the MERRA-2 forced version as SMLG-M2 and to the ERA-5 forced version as SMLG-E5.

As SnowModel-LG is not released operationally, we also calculate a climatology from the MERRA-2 forced version using data from January 2010 to December 2022 to allow operational use and to investigate the impact of using a climatology compared to inter-annually varying data. As the initial version of the SnowModel-LG climatology still has data gaps and model artifacts, such as heavily accumulated snow near coastal areas, further post-processing is applied. All data within 100 km of the coastline in the central Arctic Basin and North Atlantic as well as all data from the Canadian Archipelago are eliminated to reduce coastal model artifacts. Instead, these gaps are then filled using a low-pass Tophat kernel filter with a width of 500 km. Any remaining gaps (i.e. further than 250 km from the nearest valid data point) in the Canadian Archipelago are then filled with the mean snow depth observed in the Hudson Bay region. Finally, two low pass filtered versions of the snow field are computed: In the central Arctic Basin a tophat filter kernel with a width of 500 km is used to smooth SnowModel-LG data, while a 250 km tophat filter is applied in regions outside the central Arctic Basin to preserve finer spatial structures. Then, the low pass filtered outputs are merged and data outside the climatological sea ice mask are discarded. We call the result SMLG-M2-Clim in short.

2.3 Merged solution - mW99+SMLG

As the (modified) Warren climatology is only valid in the Central Arctic, while SnowModel-LG accumulates errors the longer the sea ice survives (i.e. is more uncertain over older ice), we combine both in a merged product. We use mW99-IC in the Central Arctic, where valid, and SMLG-M2-Clim elsewhere. For a smoother result, both are averaged in a 500 km wide band at the edge of the W99 validity mask. The use of ice charts over ice age data and the SnowModel-LG climatology are motivated by operational requirements. This solution, here called mW99+SMLG (Hendricks, 2026) has been used as the year-round snow depth product for converting radar to sea-ice freeboards in the latest CryoTEMPO Baseline-E, for both winter and summer sea

https://doi.org/10.5194/egusphere-2026-5997
Preprint. Discussion started: 20 October 2026
© Author(s) 2026. CC BY 4.0 License.

ice themes. However, this is not to be confused with the separate CryoTEMPO snow depth thematic product calculating winter snow depth from dual altimetry. In this study we test mW99+SMLG, which is available year round, and also calculate snow depth from dual-altimetry ourselves following the concept of the CryoTEMPO snow theme, but year-round (next section).

2.4 Dual altimetry - KuLa Clim

Assuming that ICESat-2 (laser, La) measures snow freeboard and CryoSat-2 (Ku-band radar, Ku) measures sea ice freeboard, their difference yields snow depth (Kacimi and Kwok, 2022; Carret et al., 2025; Landy et al., 2026b). As ICESat-2 was launched in September 2018, we build a climatology from the years 2019-2024. From ICESat-2 we use the ATL20 daily gridded snow freeboard data year-round (Petty et al., 2025b). For CryoSat-2, we use L1b data retracked with the LARM retracker (Landy et al., 2020) for the winter months (Oct-Apr) and CryoTEMPO radar freeboard data during the summer months (May-Sep). The along-track CryoSat-2 data is binned onto the same grid as ICESat-2 for each day. During the melt season, the presence of melt ponds introduces a negative EM-bias, as the highly reflective melt ponds dominate the radar return signal, but sit lower than the average ice floe surface (Landy et al., 2022; Braakmann-Folgmann et al., 2026). Therefore, this bias is approximated as a function of sea ice roughness and melt pond fraction (Landy et al., 2022) and the gridded data is corrected for this bias. As the bias correction is snow depth dependent (Landy et al., 2022), we perform five iterations. First we calculate snow depth as the difference between ICESat-2 and CryoSat-2 freeboard data without the bias correction. Then we iteratively calculate (i) the bias correction based on the resulting snow depth and (ii) snow depth using the bias-corrected CryoSat-2 freeboard data until convergence (5 iterations needed). To cover almost all grid cells, we also apply a running mean of +/- 15 days to both the ICESat-2 and (bias-corrected) CryoSat-2 maps. Another factor we need to consider is the slower propagation speed of the radar signal through the snow pack. For this we estimate snow density ρ_s as a function of days since August 1st t following Mallett (2025):

$$\rho_s = 0.35 \cdot t + 239.78 \tag{1}$$

With this we can calculate the speed of light within the snow layer c_s with respect to the speed of light in vacuum (Ulaby and Long, 2014):

$$\frac{c_s}{c} = (1 + 0.51 \cdot \rho_s/1000)^{-1.5} \tag{2}$$

And we can correct for the slower speed of the radar signal in the snow layer when calculating snow depth h_s:

$$h_s = (fb_{La} - fb_{Ku}) \cdot \frac{c_s}{c} \tag{3}$$

Here, we take the difference for each day from 1 January 2019 to 31 December 2024. As a final step, we build a daily climatology from the 6 years of overlapping data and abbreviate it KuLa Clim.

https://doi.org/10.5194/egusphere-2026-5997
Preprint. Discussion started: 20 October 2026
© Author(s) 2026. CC BY 4.0 License.

3 Reference data

To validate the snow products, we use buoys measuring snow depth, airborne and helicopter-borne measurements of freeboard and thickness as well as mooring data of sea ice draft. The validation data cover different regions and ice types and all months including the more challenging summer period of May to September (see Figure 1). In addition, melt freeze indicators from passive microwave data are used to investigate the timing of snow ablation.

3.1 Buoy measurements of snow depth

We use snow depth estimates from snow buoys and ice mass balance (IMB) buoys of 126 buoys in total. This dataset consists of snow buoys available from meereisportal.de (Nicolaus et al., 2017) and IMB buoys processed by Preußer et al. (2025), Lei et al. (2021) and Salganik and Landy (2025) covering the years 2010-2020 (see Figure 1). The snow buoys have four ultrasonic sensors installed around a central pole measuring the distance to the snow surface. Similarly, the IMB buoys measure the distance to the snow surface at one point and record ice thickness with an additional sensor under the ice. The buoys drift with the sea ice floe on which they were deployed, until the floe melts or until the sensor falls over or fails. We set negative snow depth measured by the buoys to zero, assuming this indicates a fall over or tilt of the system. The advantages of buoy observations are that they offer high temporal coverage, provide a direct in situ measurement of snow depth, and cover various areas of the Arctic Ocean (see Figure 1). On the other hand, the measurements only represent snow depth at one/four points within $\sim$ 1x1 m, which is hard to compare to the much larger-scale snow products, as snow depth tends to be very heterogeneous even on small spatial scales and on the same ice floe (Sturm et al., 2002). We include the buoys in our comparison, as they are the only means of in situ snow depth measurement in summer, but keep in mind their limited ability to represent large-scale snow depth and focus on the temporal evolution (Petty et al., 2025a; Wever et al., 2021; Zhou et al., 2021).

3.2 Airborne and helicopter-borne measurements of sea ice freeboard and thickness

We use airborne measurements from two Operation IceBridge (OIB) campaigns measuring snow freeboard (sea ice freeboard + snow depth), various IceBird campaigns measuring total SIT (ice thickness + snow depth) and the MOSAiC (Multidisciplinary drifting Observatory for the Study of Arctic Climate) helicopter measurements of total SIT. Figure 1 shows an overview of the flight tracks and when they were acquired.

NASA's OIB campaigns took place on 16 and 19 July 2016 and 24 and 25 July 2017. The OIB laser scanner freeboards were derived from raw height observations using the method described in the supplementary material 1 of Dawson et al. (2022). OIB observations have a footprint of 40 meters.

The Alfred-Wegener-Institute (AWI) conducted a series of airborne electromagnetic bird flights (AEM) in spring and summer 2016-2024 (24 July-1 August 2016, 2-8 April 2017, 13-28 August 2017, 31 July-13 August 2018, 2-10 April 2019, 5-10 August 2023, 12 April-6 May 2024 and 26 July-7 August 2024, Belter et al. (2021); Jutila et al. (2024); Krumpen et al. (2025)). This dataset includes total (snow plus sea ice) thickness observations with a footprint of 10s meters.

https://doi.org/10.5194/egusphere-2026-5997
Preprint. Discussion started: 20 October 2026
© Author(s) 2026. CC BY 4.0 License.

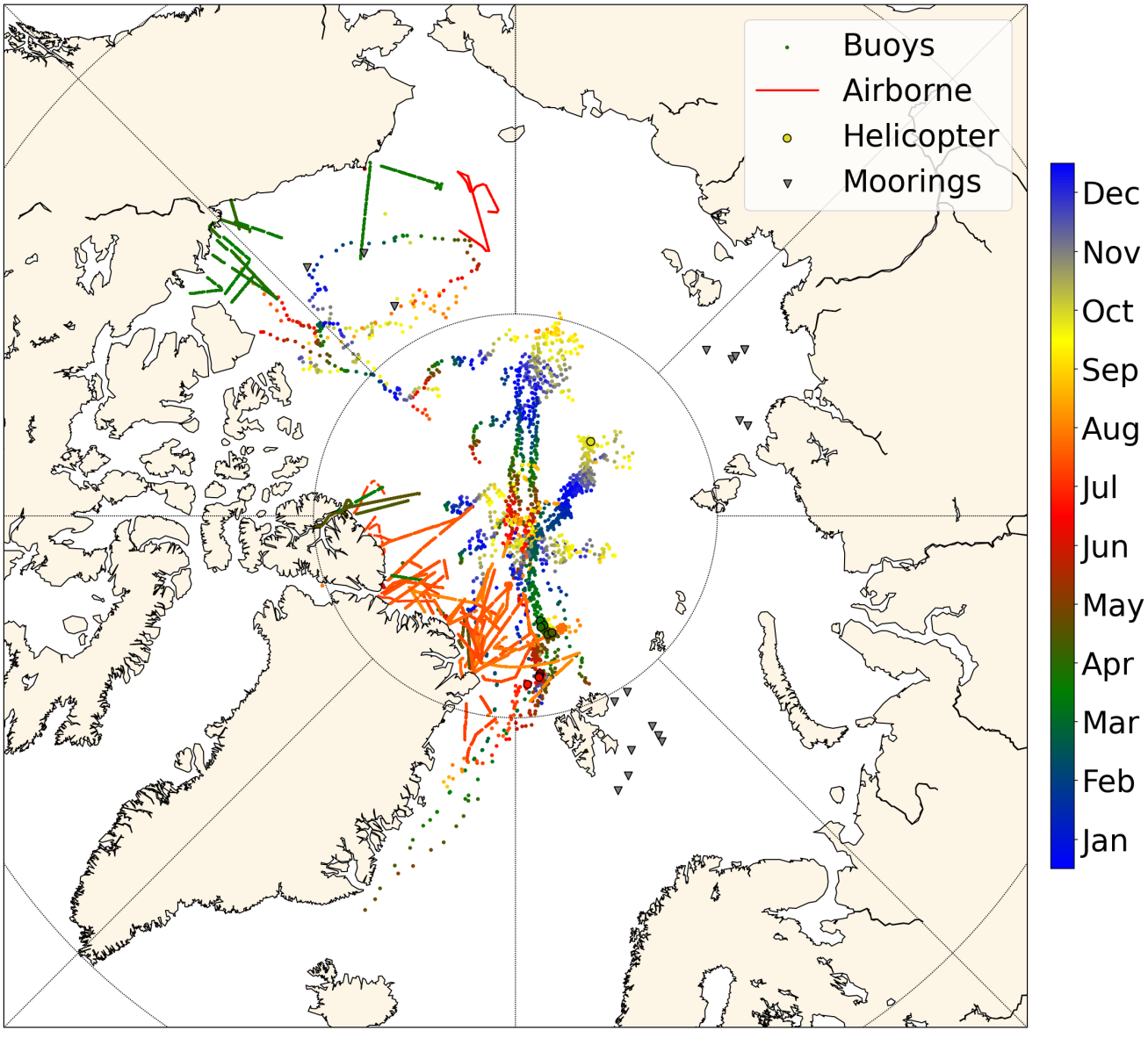


Figure 1. Validation data used for comparison: Mooring data from the Beaufort, Laptev and Barents Sea are available year-round (when sea ice covered) and marked by grey triangles. Airborne and helicopter-borne observations as well as buoy data are colour coded by the time of acquisition. As the MOSAIC helicopter data covers smaller areas and was collected at the same locations and times as the MOSAIC buoys, the data overlap, but can be differentiated when zooming in.

https://doi.org/10.5194/egusphere-2026-5997
Preprint. Discussion started: 20 October 2026
© Author(s) 2026. CC BY 4.0 License.

Finally, we also use helicopter-borne electromagnetic bird flights (HEM) from the MOSAIC campaign (von Albedyll et al., 2021). These flights took place on 14 October 2019, 4 April 2020, 10 April 2020, 17 April 2020, 26 April 2020, 30 April 2020, 19 June 2020, 21 June 2020, 22 June 2020 and 7 July 2020 and have a footprint of several meters.

3.3 Mooring measurements of sea ice draft

Upward-looking sonar (ULS) and Acoustic Doppler Current Profiler (ADCP) data of sea ice draft are used covering three locations in the Beaufort Sea, seven locations in the Laptev Sea and eight locations in the Barents Sea. This yields a good spatial distribution of validation datasets, covering several first-year ice areas, and hence complementing the airborne data over thick and rough MYI (see Figure 1). Temporally, the ULS data from the Beaufort Gyre Exploration Program (BGEP, https://www2.whoi.edu/site/beaufortgyre/) contain data from 2011-2023 capturing the full seasonal evolution over more than a decade. Hence, they allow for an assessment across all stages of cold winter snow, snow melt, melt pond formation, draining and re-freezing. In the Laptev Sea (Alfred-Wegener-Institute, Belter et al. (2019, 2020)) and Barents Sea ((Onarheim et al., 2024; Divine et al., 2025)), the ice cover disappears earlier (between May-July depending on the year and mooring location), but as the airborne data mainly cover July-August, this makes a valuable addition to the overall dataset and balances the temporal coverage across the so far unvalidated summer months as well as the spatial coverage by extending more into the marginal ice zones. Data from the Laptev Sea moorings is available between 2010 and 2016. Six of the Barents Sea mooring locations use ULS, which were deployed between 2013 and 2022 and the remaining two are ADCP sensors, which recorded data between 2018 and 2021.

3.4 Melt onset timing

A key difference between the various snow depth products is the timing of snow melt onset and freeze-up, i.e. when snow ablation and accumulation start. Therefore, we compare the snow depth products to melt and freeze indicators derived from passive microwave observations (Steele et al., 2026) following Markus et al. (2009). This data yields four dates for each 25 km grid cell and each year (1979-2023): early melt onset, continuous melt onset, early freeze onset and continuous freeze onset. Early melt refers to the first day when melt is detected. Continuous melt and early freeze onset are the first and last days of the main melt period.

4 Methods for comparison

To inter-compare the different snow depth products and validate them against in situ data, we need to harmonise their spatio-temporal sampling and calculate the same geophysical variables (e.g. SIT) with different snow depth estimates.

4.1 Sampling and gridding

As each snow depth product comes at a different spatial resolution and projection, we grid them on a common 80 km polar stereographic grid (+proj=stere +lat_0=90 +lat_ts=70 +lon_0=0 +x_0=0 +y_0=0 +datum=WGS84 +units=m). For Warren we

https://doi.org/10.5194/egusphere-2026-5997
Preprint. Discussion started: 20 October 2026
© Author(s) 2026. CC BY 4.0 License.

evaluate the polynomial directly at the grid locations. SMLG, the ice age data and ice charts and the KuLa climatology (which is originally computed on the ICESat-2 grid) are regridded (using the xESMF conservative_normed regridder, Zhuang et al. (2022)). Target grid cells are assigned a value when at least 50% of their contributing area contains valid data and in this case the value is the area-weighted mean. Also the airborne and helicopter-borne data are averaged onto the same 80-km grid. Due to the smaller spatial coverage of the helicopter data, each flight day yields only one data point.

In terms of temporal sampling, we resample each snow depth product daily. For monthly climatologies (W99 and SMLG-M2 Clim), we assume the values represent the 15th of each month and perform a linear interpolation. For the ice charts and ice age data we perform a nearest neighbor interpolation between available dates (usually weekly).

When comparing to snow depth observations from the buoys, we average both the snow depth and in situ data at 5 day intervals to reduce noise. For comparisons of sea ice freeboard, SIT and draft, which require CryoSat-2 freeboard data together with snow depth estimates, we sample all data biweekly (twice a month), to avoid data gaps in the CryoSat-2 data. We also employ a larger search radius of 100-200 km (depending approximately on the local mean ice drift speed) when comparing to validation data to account for the larger spatial resolution of the satellite and snow data as well as ice drift over the two weeks.

4.2 Sea ice freeboard, SIT and draft

One key application of snow depth products is their use in converting satellite radar or laser freeboard observations to sea ice freeboard, SIT and sea ice draft. Therefore, we also test the impact of the various snow depth products on this conversion together with CryoSat-2 radar freeboard. Just as for the KuLa climatology, we use LARM retracked CryoSat-2 observations in winter and the CryoTEMPO summer sea ice product for May-September. To convert radar freeboard h_{rfb} to sea ice freeboard h_{fb}, we correct for the slower propagation speed of the radar signal in the snow layer using

$$h_{fb} = (h_{rfb} + \Delta h_{rfb}) + \delta_p h_s (\frac{c}{c_s} - 1) \tag{4}$$

where Δh_{rfb} is the bias-correction added in the summer month to compensate for a melt pond induced EM bias ((Landy et al., 2022)). The bias correction, $\frac{c}{c_s}$ and ρ_s are calculated as described in section 2.4. The penetration depth factor δ_p is set to 0.9 following Landy et al. (2022). For snow depth h_s we use the various snow depth estimates. Instead of the Mallett (2025) parametrisation of ρ_s we also tested using the snow density estimates from Warren and SMLG and found little difference. Since KuLa does not yield a density estimate and to separate the impact of the snow depth estimates, we therefore decided to use a common snow density parametrisation for all snow depth estimates.

Then we convert sea ice freeboard to SIT assuming hydrostatic equilibrium, where sea water density ρ_w = 1024 kg/m^3:

$$SIT = \frac{h_{fb}\,\rho_w + h_s\rho_s - h_s\rho_w + \delta_p\,h_s\,\rho_w + 1000\,h_{mw}}{\rho_w - \rho_i} \tag{5}$$

For sea ice density ρ_i and the additional melt water loading term h_{mw} we employ the new parameterisations by Landy et al. (2026a).

https://doi.org/10.5194/egusphere-2026-5997
Preprint. Discussion started: 20 October 2026
© Author(s) 2026. CC BY 4.0 License.



And finally, draft is simply calculated as SIT minus sea ice freeboard.

$$draft = SIT - h_{fb} \tag{6}$$

For the OIB campaigns measuring snow freeboard, we derive sea ice freeboard by subtracting the various different snow depth products. Similarly, SIT is derived from the total thickness measured by IceBird and the MOSAIC helicopter surveys by subtracting the various snow depth estimates from total thickness. This means that the snow depth estimates are used twice in the airborne comparison - once to derive sea ice freeboard and SIT from CryoSat-2 radar freeboard observations and once to reduce the total freeboard and total thickness measurements by the airborne and helicopter data.

5 Results and Discussion

We start with an intercomparison of the various snow depth products to understand their characteristics, where they agree and where they differ. Then we compare them to snow depth observations from buoys before assessing the impact of the different snow depth estimates on the resulting SIT and draft. Finally, we discuss the applicability of KuLa dual-altimetry snow depth for the summer months.

5.1 Intercomparison of snow products

First, we assess the spatial patterns and temporal evolution of the various snow depth products and intercompare them. Figure 2 shows monthly maps of snow depth for 2019. In addition to the individual products we also plot the mean and standard deviation of all available products per grid cell to assess their agreement and differences. The last column indicates the melt/freeze state of the snow based on passive microwave data (Steele et al., 2026). All data are cut to 50 % sea ice concentration using OSISAF-450 ((Lavergne et al., 2019)) to show the same ice covered areas of 2019. For the (modified) Warren climatology, it is apparent that the extrapolated snow depth is overestimated on both sides of Greenland and negative values occur in the Kara Sea. Therefore, we only use the data constrained by actual measurements (opaque in Figure 2) in the following analysis.

As anticipated, the Warren climatology yields the highest snow depth of all products throughout the year and appears very smooth without local variations due to the simple polynomial. The two modified Warren climatologies clearly reflect the spatial patterns of the MYI boundary. The general pattern is similar using either the ice age product or ice charts, but they differ in the exact outline of the MYI edge and mW99-IA exhibits more local variation in areas of mixed ice types (e.g. North of Svalbard in February). mW99+SMLG and mW99-IC are the same in the Central Arctic and only differ in areas where mW99-IC needs extrapolation. In those areas, on the other hand, mW99+SMLG is equal to SMLG-M2 Clim (next column). Regarding the SMLG-based products, SMLG-M2 and SMLG-E5 show minimal differences up to May. However, they strongly disagree in June, when the ERA5 forcing already melts away the entire snow cover in large parts of the Arctic and yields zero snow depth across the whole Arctic for both July and August. In contrast, the MERRA2 forcing leads to slower snow melt, with most areas still exhibiting a significant snow cover in June, roughly half of the Arctic being snow free in July and some minor snow accumulation already happening in August. The higher snow depth from SMLG-M2 then persists throughout autumn.

https://doi.org/10.5194/egusphere-2026-5997
Preprint. Discussion started: 20 October 2026
© Author(s) 2026. CC BY 4.0 License.

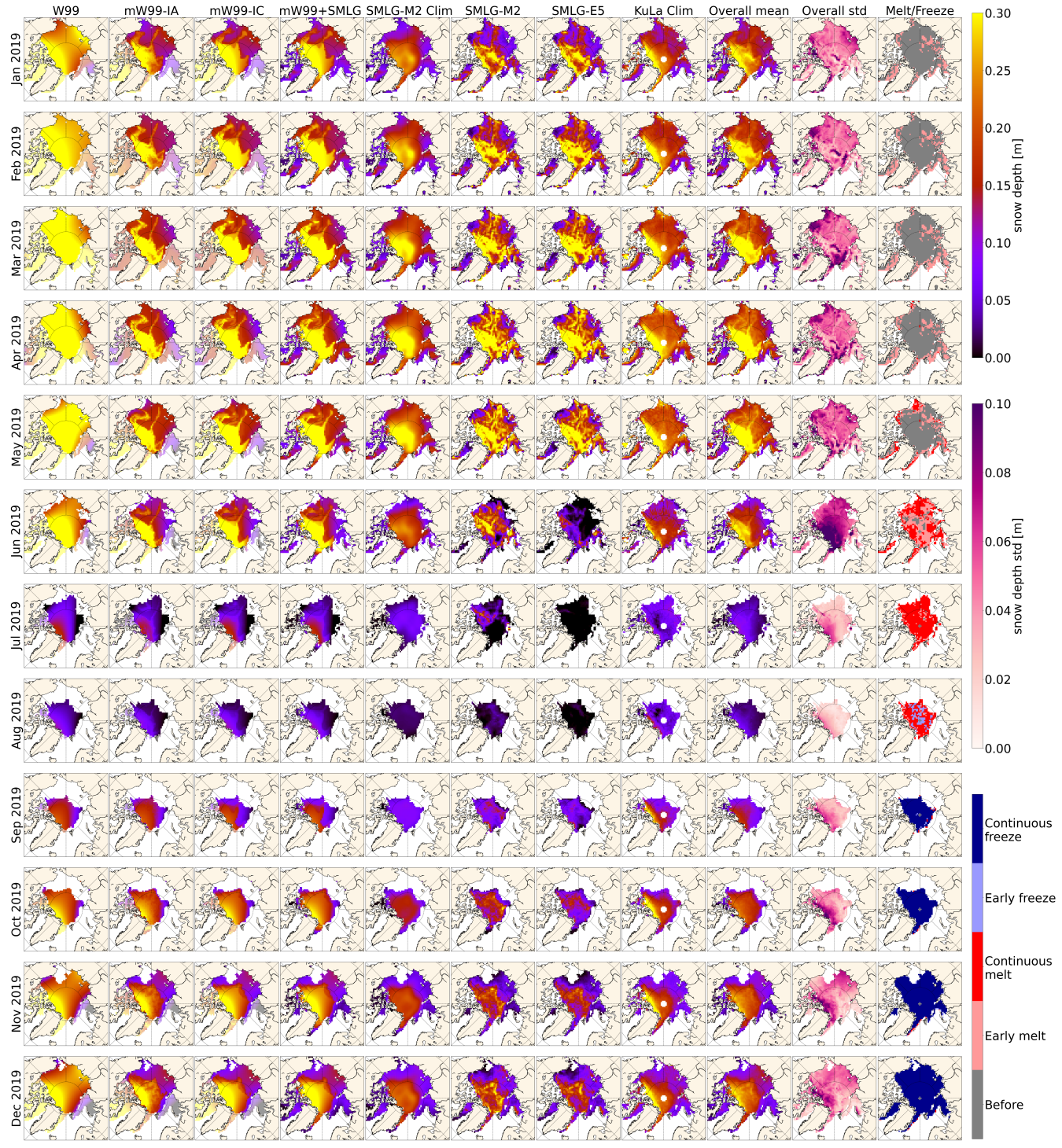


Figure 2. Monthly maps (15th of each month) of snow depth from the various products as well as their mean and standard deviation for 2019. The last column shows the melt/freeze state as indicated by Steele et al. (2026). For the Warren climatologies we plot data that is extrapolated beyond the area where the climatology was defined as semi-transparent. In the following analysis we only use the valid (opaque) data, though.

https://doi.org/10.5194/egusphere-2026-5997
Preprint. Discussion started: 20 October 2026
© Author(s) 2026. CC BY 4.0 License.

SMLG-M2 Clim is based on SMLG-M2 and generally shows a similar average snow depth, however with significantly less spatial variation and naturally no inter-annual variation. We can also see a similar pattern of sharply higher snow depth in MYI areas from mW99-IA, mW99-IC, SMLG-M2 and SMLG-E5, that is not captured by the pure climatologies. The KuLa climatology somewhat resembles the SMLG-M2 Clim, albeit with higher snow depth North of Greenland and the Canadian Arctic Archipelago in a thinner band, whereas the highest snow depth in SMLG-M2 Clim is concentrated across the Central Arctic. Furthermore, KuLa starts accumulating snow earlier - already in August and snow depth North of Greenland and the Canadian Arctic Archipelago already reach 25-30 cm in September, whereas SMLG-M2 Clim only estimates them to be 5-10 cm.

The overall mean reflects the general patterns of spatio-temporal snow depth evolution including the higher snow depths in MYI areas. The standard deviation across all products highlights months and areas with the highest discrepancies. From January to April an area North of Svalbard indicates high discrepancies between the products, as SMLG predicts lower snow depth, while the Warren-based products estimate snow depth to be high. June is the month with the highest variation amongst the products, at a time when snow depth is around the annual peak and the timing of snow ablation can vary between datasets. In contrast, August is the month with lowest standard deviation, as snow depth is also lowest. These are also the months, where the in situ observations by Warren et al. (1999) show the highest (June) and lowest (August) root mean squared error of the fit and interannual variability. In autumn the biggest discrepancies are North of Greenland and the Canadian Arctic Archipelago, where the Warren-based products and KuLa Clim estimate snow depth to be high, while the SMLG products show less of a spatial gradient. If we assume that the in situ observations from Warren et al. (1999) are still representative for this area of thick MYI, this would indicate an underestimation of SMLG in this area and question the decision to convert all remaining snow to ice on 1st August, as the observations by Warren et al. (1999) suggest that some snow survives the summer. On the other hand, the KuLa difference is especially affected by freeboard biases and discrepancies in this area as discussed in section 5.5. The average standard deviation between the products is around 4 cm year-round and for both the winter (Oct-Apr) and summer months (May-Sep) average. June sticks out as the most uncertain month in terms of average discrepancy between products (7 cm), whereas August has the lowest discrepancy (2 cm).

Finally, we also assess the agreement with passive-microwave based estimates of snow melt and freeze onset. May is the first month where continuous melt occurs around the margins and these areas either lose ice completely by mid June (Chukchi Sea) or show lower snow depth in mid June (Fram Strait). For 15th June the passive microwave data suggests a patchy mix of no melt yet, early melt and continuous melt, before the whole Arctic experiences continuous melt by mid July. We also observe the clearest reduction in snow depth across all products between June and July - except for SMLG-E5, where the main drop already occurs from May to June. On 15th August, parts of the Central Arctic start to experience early freeze onset and by 15th September essentially the whole Arctic has reached a continuous freeze stage again. This matches with all snow products starting to accumulate snow again between August and September.

To learn more about the seasonal cycle of the various snow depth products, we average all of them across the whole Arctic and all available years (2010-2021 for SMLG, 2019-2024 for KuLa and 2010-2024 otherwise, Figure 3). To avoid differences due to coverage, we only keep areas where all products have valid data (i.e. the Central Arctic, where Warren is defined) and

https://doi.org/10.5194/egusphere-2026-5997
Preprint. Discussion started: 20 October 2026
© Author(s) 2026. CC BY 4.0 License.

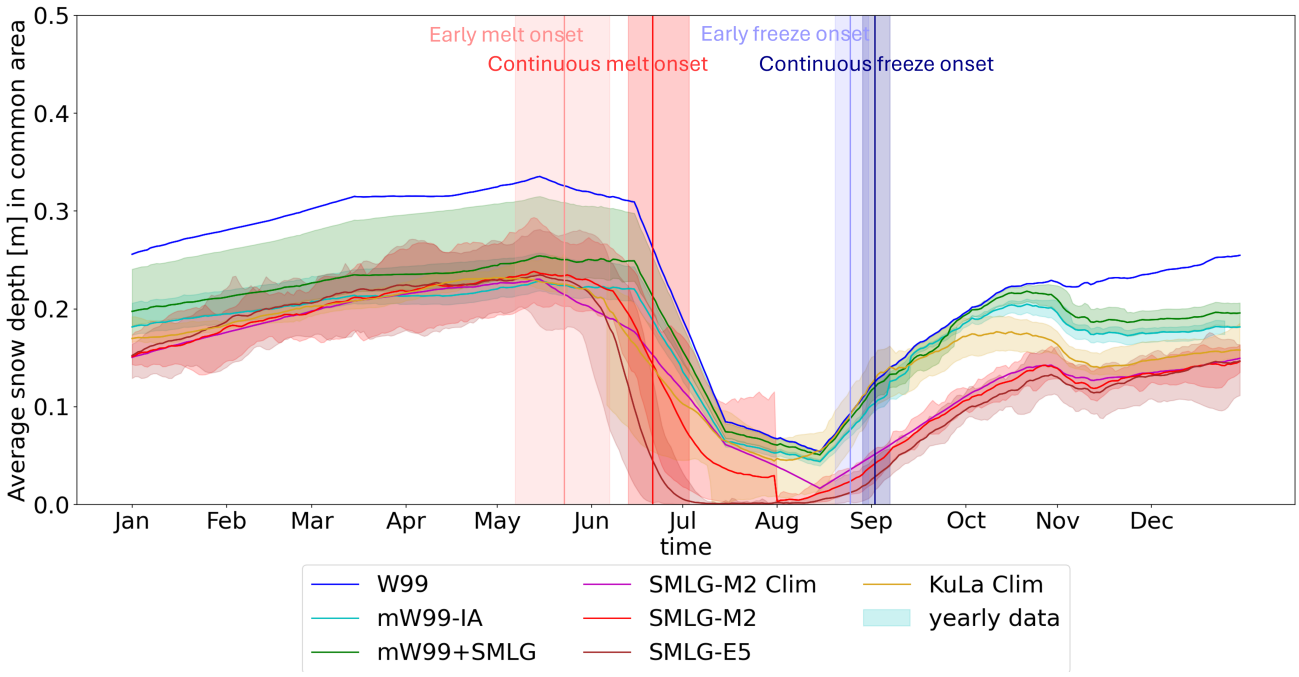


Figure 3. Temporal evolution of snow depth averaged in the common areas where all products contain valid data across all years. This is mainly the Central Arctic, where the Warren climatology is well defined. Therefore, mW99-IC is equal to mW99+SMLG and not shown separately. Thin, semi-transparent lines represent individual years and bold lines represent the average of the years 2010-2024, except for SMLG it is 2010-2021 and 2019-2024 for KuLa. The decrease in November is due to new ice formation (sharp increase in valid grid cells), which lowers the average snow depth.

where sea ice concentration is > 50 % across all years. Again, we find that W99 yields the highest snow depths by some margin - only in the second half of August the KuLa climatology is around as high as W99. The second highest are mW99-IC and mW99+SMLG, which are identical in the analysed area. Apart from a short period in September, these are consistently higher than mW99-IA, showing that the ice charts define larger areas as MYI than the ice age product. The ice charts also have a larger interannual variation (spread of the green shading in Figure 3). Throughout winter and early spring all SMLG products and KuLa agree very well and also mW99-IA agrees with them between February and May. In contrast, there are clear differences in the summer months, with SMLG-E5 declining earliest and fastest. SMLG-M2 and KuLa agree on the melt onset timing, but the drop in SMLG-M2 is steeper and KuLa retains ∼5 cm of snow throughout the summer. SMLG-M2 also shows ∼3 cm snow remaining by the end of July, which then becomes superimposed ice on 1st August according to the model configuration (Liston et al., 2020). Where monthly climatologies were generated and interpolated linearly, we observe these artefacts mainly in the dynamic melt season. Overall, the timing of all snow products agrees fairly well with the passive microwave derived indicators of early and continuous melt onset, as they all start to decline between early melt onset and continuous melt onset and shows the steepest gradient around the continuous melt onset indicator - again with the exception of SMLG-E5 that is mostly

https://doi.org/10.5194/egusphere-2026-5997
Preprint. Discussion started: 20 October 2026
© Author(s) 2026. CC BY 4.0 License.

gone by continuous melt onset. The observed snow accumulation starts in August for all products, which is slightly earlier than the freeze onset indicators. In October the KuLa Clim snow depth is more or less stable, while all other products increase. An investigation of the input data shows that this comes from the ICESat-2 data, where total freeboards increase until October each year, then stagnate for about a month before shortly dropping between late October and early November. Afterwards ICESat-2 freeboards steadily increase again. The KuLa evolution in October might therefore be an artefact in the ICESat-2 processing and should be investigated further. Before the drop the KuLa Clim agrees more closely with the Warren products, but then approaches the SMLG products in November and December. All datasets show a period of decreased average snow depth around late October/early November due to the extensive formation of snow-free new sea ice. Investigating the number of valid grid cells that are used for the average confirms that this period corresponds to the fastest sea ice growth period across all years.

5.2 Validation against snow and ice buoys

Having analysed the different characteristics of the various snow depth products, we now compare them to in situ observations of snow depth from snow and ice buoys. Overall, we find low biases for most products across all seasons (Table 2). SMLG-M2 and also its corresponding climatology yield no bias, but also SMLG-E5, KuLa Clim and mW99-IA yield biases of only 2 cm (plus or minus). The Warren climatology yields the highest bias of +6 cm. The RMSE is significantly higher for all products and varies from 14-16 cm. Correlations are generally low and vary from 0.11 (SMLG-M2 Clim) to 0.29 (mW99-IA).

We also analyse the evolution of snow depth since buoy deployment by setting the initial snow depth to zero for both the buoy and snow products (Figures A1,4, Table 2). Only buoys with > 10 data points (i.e. recording for > 46 days) are considered. Doing so, we can no longer analyse the agreement in absolute snow depth, but we mitigate uncertainties due to the specific deployment location and focus only on changes in snow depth over time. While the comparison of absolute values yielded an average correlation of 0.22, the relative change analysis increases it to an average of 0.51 (Table 2). mW99-IA and SMLG-M2 yield the highest correlation in relative change. Also visually, we find that the snow products and buoys agree on the main patterns (stable / increase / decrease), but the snow products behave more similarly amongst themselves (Figure A1). Looking at the distribution of snow depth evolution, the buoys show a long tail of snow accumulation, while most snow depth products are more symmetric (Figure 4). This most likely reflects the difference in scale between buoys and the snow products, with a higher probability that a buoy captures more extreme accumulation than a product with 10+ km resolution. The KuLa Clim yields by far the narrowest distribution, underestimating snow accumulation and ablation. Both versions of SMLG exhibit the widest spread, capturing both extremes of snow accumulation and melt, albeit still with some scatter.

The biggest shortcoming of buoy comparisons is their limited representativeness (Petty et al., 2025a). While each buoy only gives a point measurement (or an average of four measurements within 1 m^2), most snow products are developed at km-scales. The snow cover is also known to be highly heterogeneous even on small spatial scales (Sturm et al., 2002). Hence, this mismatch in spatial scales is a major limitation. To somewhat compensate for it, we select and average the snow depth measurements of 25 buoys that were deployed close to each other during the MOSAIC campaign. The spread of the individual buoys confirms the large variability within a small area (Figure 5). Between October and January, SMLG-E5 is the only snow

https://doi.org/10.5194/egusphere-2026-5997
Preprint. Discussion started: 20 October 2026
© Author(s) 2026. CC BY 4.0 License.

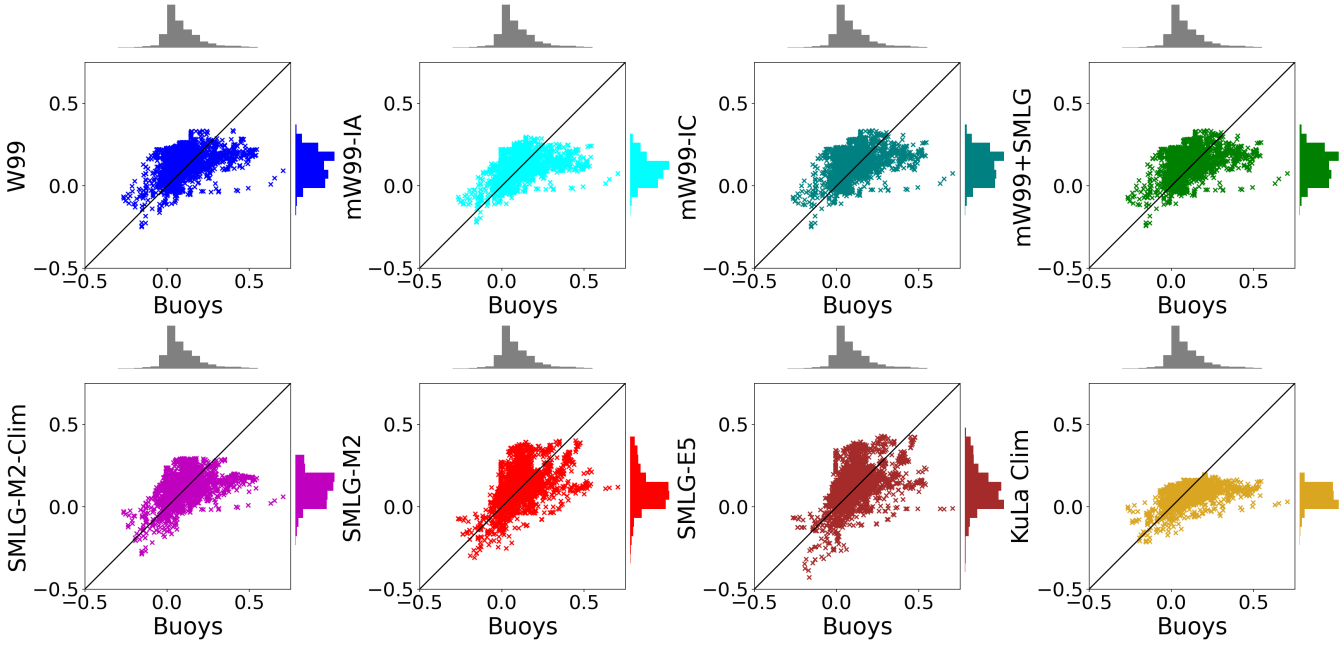


Figure 4. Comparison of relative snow depth evolution since buoy deployment [m] versus the various snow depth estimates [m]

product slightly underestimating the buoy mean, while the KuLa Clim is more or less spot on and the remaining snow products exhibit a slight overestimation. From January onward all products overestimate snow depth compared to the buoy mean, but stay within the spread of the individual buoy measurements until July. Transect data from MOSAIC is consistently higher than the buoy average (Itkin et al., 2023), and therefore closer to the various snow depth products. The transects indicate average snow depths of around 20 cm in December and around 25 cm in April, May, but no measurements are available for the most critical melt onset period of June (Figure 7 of Itkin et al. (2023)). Therefore, we use the continuous buoy measurements and focus more on the relative evolution. The general behaviour and differences in this case study are similar to the overall mean (Figure 3), but thanks to the buoys we can now determine which evolution best matches reality. The buoy mean snow depth drops sharply at the end of May, somewhat stabilizes in early June and the mean reaches zero in early July. However, a lot of individual buoys already reach zero end of June. Both SMLG versions and the SMLG-M2 Clim start declining slightly before the main drop in mean buoy snow depth. SMLG-E5 is the first one to reach zero snow depth - together with the first buoys dropping to zero, but significantly before the buoy mean. SMLG-M2 captures the timing of snow melt best, closely following the buoy mean. The corresponding climatology declines a bit too slowly and has too thick snow in April. The KuLa climatology and all versions of the (modified) Warren climatology, including mW99+SMLG, estimate a later snow melt onset than recorded by the buoys, but KuLa is still only slightly delayed, whereas the Warren-based products are almost one month late. This mainly indicates that snow was melting earlier than usual in the specific area in 2020 and a general limitation of climatologies is that they do not capture inter-annual anomalies, in either depth or timing of seasonal transitions. If the KuLa Clim would reach zero snow depth, it would actually still capture the full snow melt quite well. However, it levels out around

https://doi.org/10.5194/egusphere-2026-5997
Preprint. Discussion started: 20 October 2026
© Author(s) 2026. CC BY 4.0 License.

end of June and stays at about 5 cm throughout summer, highlighting the mid-summer bias evident in Figure 2. Finally, the W99, mW99-IC and mW99+SMLG essentially show the same evolution, as the ice charts mark the area as MYI. All three curves (mW99-IC not shown) reveal by far the highest snow depth throughout, drop latest and still retain 10 cm of snow at the end of July. In contrast, the ice age product indicates mixed ice types and therefore mW99-IA yields lower snow depth, but still with a late decline and not reaching zero. Overall, we find that SMLG-M2 captures the melt evolution best, followed by KuLa Clim and SMLG-M2 Clim but with a slight offset in absolute snow depth. SMLG-E5 drops earliest, which is representative for areas of lower snow depth, but too early compared to the mean.

Plotting the agreement between the mean of the MOSAIC cluster and the various snow products at 5-day intervals confirms these observations (Figure 6). SMLG-M2 mostly follows the 1:1 line especially for lower snow depth measurements as snow melts to zero. For SMLG-E5 we can clearly see how the model predicts snow ablation to zero before the buoy observations and the opposite behaviour is seen from all other products at smaller or greater extent. KuLa Clim and SMLG-M2 Clim exhibit more or less a parallel line to the 1:1 line for the melt period (downward pointing triangles in Figure 6), constantly overestimating snow depth (potentially because snow depth was lower than in other years and these products are climatologies).

Overall, SMLG-M2 shows the best agreement with all the buoys in terms of melt onset timing, capturing the full range of values, no absolute bias and a high correlation. mW99-IA also shows high correlation, but agrees much worse in terms of melt onset timing for the MOSAIC buoys. KuLa Clim and SMLG-M2 Clim do well within the limitations of being climatologies and SMLG-E5 yields high correlations and good overall agreement, but melts too early compared to the buoys.

5.3 Validation of freeboard and SIT against helicopter and airborne data

One of the main applications of snow depth estimates is the calculation of sea ice thickness. Therefore, we also analyse the impact of the various different snow depth products on the resulting SIT. However, we have to keep in mind that several other observations and assumptions with non-negligible uncertainties affect SIT estimates and may mask the effect of snow depth. In particular, uncertainties in CryoSat-2 radar freeboard and ice density can contribute substantially to the overall uncertainty in SIT (Ricker et al., 2014; Sievers et al., 2024). Both have higher uncertainties in the melt season, just like snow depth. As the focus of this paper is on the much less explored summer season, the selected OIB campaigns are exclusively from the summer months (July, see Fig. 1), most of the IceBird campaigns considered here were also conducted in summer (late July - August), but data from April is included, too. Finally, we use helicopter-borne surveys from the MOSAIC campaign covering October - July with most flights conducted in April and June (see Fig. 1).

During the OIB campaigns, sea ice freeboard was measured with an airborne lidar system and 35 grid cells were covered. Snow depth affects the OIB laser scanner freeboard, because this is the total freeboard (e.g. sea ice freeboard + snow depth). It also affects the conversion of CryoSat-2 measured radar freeboard to sea ice freeboard through the delay in the propagation speed through the snow layer. Hence, we test the impact of different snow depth products on the agreement between CryoSat-2 derived and OIB derived sea ice freeboard. Our comparisons show clear differences when different snow depth products are used together with the same CryoSat-2 radar freeboard data (Table 2). While mW99-IC and mW99+SMLG (which are the same in the Central Arctic where the data was collected) yield no bias at all, using SMLG-M2 results in an 11 cm bias. The

https://doi.org/10.5194/egusphere-2026-5997
Preprint. Discussion started: 20 October 2026
© Author(s) 2026. CC BY 4.0 License.

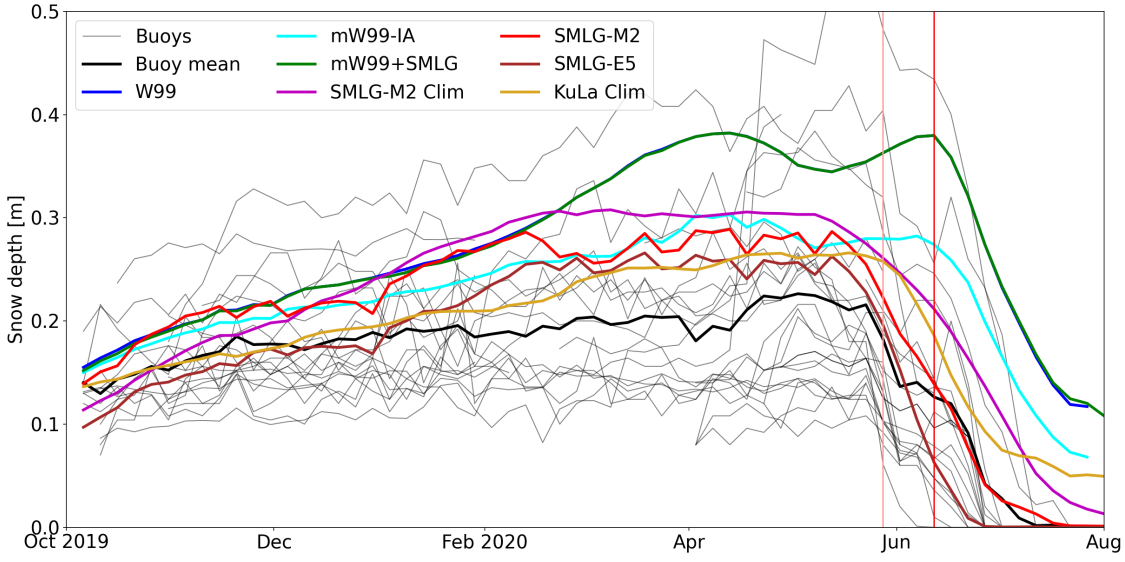


Figure 5. Temporal evolution of snow depth as measured by the individual MOSAIC buoys (thin grey lines), their average (bold black line) and the different snow depth products (coloured lines) from October 2019 to August 2020. The light red and red vertical lines indicate early and continuous melt onset derived from passive microwave observations.

RMSE varies between 6 cm for the KuLa Clim and 12 cm for both versions of SMLG. The Pearson correlation coefficient lies between 0.72 for both versions of SMLG and 0.84 for W99, mW99-IC and mW99+SMLG. For comparison we also calculate sea ice freeboard assuming no snow and this gives the same results as SMLG-M2. Hence, this comparison suggests that snow was still present in July, when the OIB flights were conducted - unless the assumption of snow compensates other biases in the CryoSat-2 radar freeboard. In any case, the combination of CryoSat-2 freeboard and a Warren derived snow product (or KuLa Clim) yields sea ice freeboards that agree significantly better with airborne measurements than assuming no snow or using a SMLG derived product.

Next, we study the impact of different snow depth solutions on SIT by comparing with IceBird flights (Figure 7). We have 227 data points from IceBird out of which 216 are valid for the Warren products. For IceBird we generally find worse agreement independent of which snow product is used. The lowest bias of -0.66 m and RMSE of 1.20 m are achieved in combination with W99. mW99-IC yields the highest correlation coefficient of 0.49. Just like for OIB, the SMLG derived products perform worse. However, assuming no snow is worst (bias -1.50 m, RMSE 1.86 m, correlation 0.09, Table 2) and using any snow product notably improves the correlation. In all cases, CryoSat-2 underestimates SIT compared to IceBird. Higher snow depth estimates increase the SIT estimate and hence agreement with IceBird. However, the fact that W99 still underestimates SIT indicates that other biases from CryoSat-2 freeboard and ice density impact the comparison over these especially ridged,

https://doi.org/10.5194/egusphere-2026-5997
Preprint. Discussion started: 20 October 2026
© Author(s) 2026. CC BY 4.0 License.

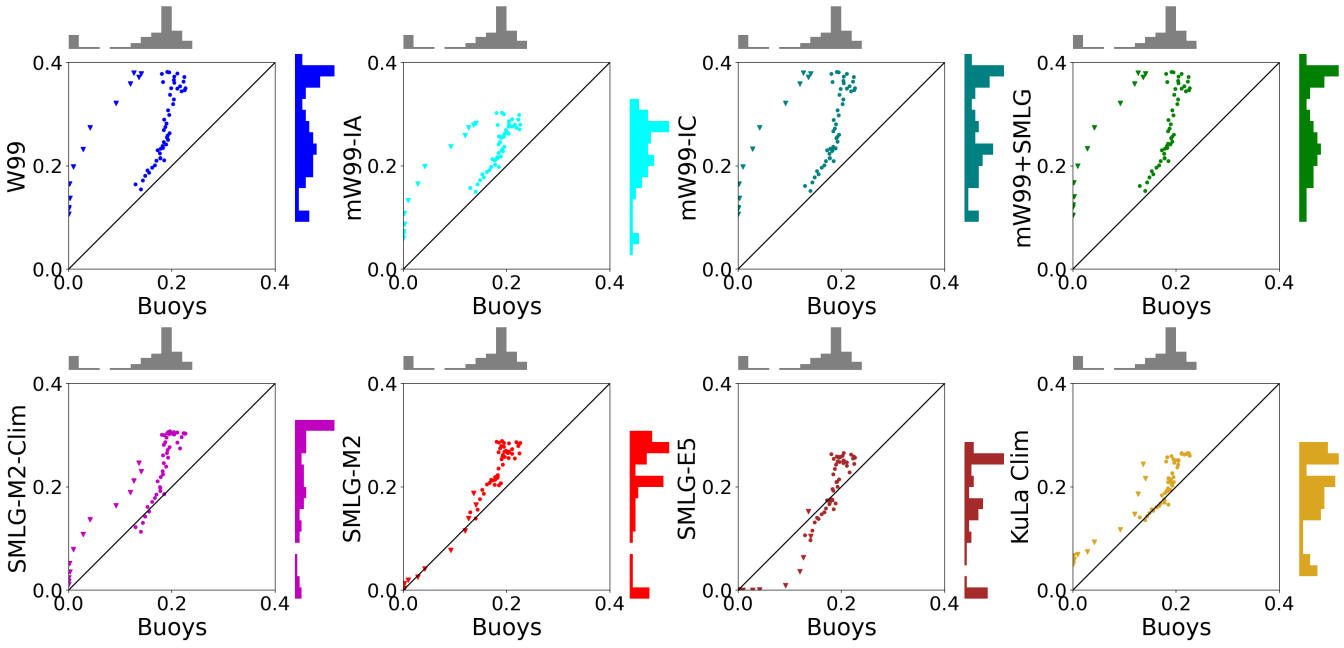


Figure 6. Comparison of mean snow depth measurements from MOSAIC buoys [m] versus the various snow depth estimates [m]. Downward pointing triangles indicate the melt period from 28th May onward.

challenging areas and higher snow can compensate some of this, but it is questionable whether higher snow depth than W99 are reasonable.

Finally, we investigate the helicopter-borne SIT estimates from the MOSAIC campaign. Due to the smaller reach of the helicopter and the large CryoSat-2 grid cells, each helicopter flight yields exactly 1 data point and n=10 in total. As the data spans various seasons, assuming no snow is clearly worse than any of the tested snow depth products in terms of bias and RMSE. However, the correlation is indeed better than for SMLG-M2, SMLG-E5 and KuLa Clim, indicating that these products introduce patterns that mask the skill of pure CryoSat-2 freeboard estimates. W99, mW99-IC and mW99+SMLG achieve the highest correlation of 0.92, while mW99-IA yields the lowest bias of -0.03 m and RMSE of 0.22 m. Interestingly, there are strong differences between mW99-IA and mW99-IC as the ice age product indicates FYI while the ice chart identifies the area as MYI. While the camp was established on second-year ice, large FYI areas evolved around the camp during the drift (Nicolaus et al. (2022)).The SMLG-M2 climatology performs significantly better than SMLG-M2 and SMLG-M2 still performs better than SMLG-E5. The KuLa Clim estimates are third best in terms of bias and RMSE, whereas the correlation is worse than most other products and only outperform SMLG-M2 and SMLG-E5. Overall, we find that the combination of CryoSat-2 freeboard and a Warren derived snow product yields better agreement with airborne measurements than assuming no snow or using a SMLG derived product. The KuLa Clim estimates are mostly in between the Warren and SMLG derived estimates.

https://doi.org/10.5194/egusphere-2026-5997
Preprint. Discussion started: 20 October 2026
© Author(s) 2026. CC BY 4.0 License.

	No snow	W99	mW99-IA	mW99-IC	mW99+SMLG	SMLG-M2 Clim	SMLG-M2	SMLG-E5	KuLa Clim
snow depth [m]									
Buoy bias		0.06	0.02	0.05	0.05	0.00	0.00	-0.02	-0.02
RMSE		0.16	0.14	0.16	0.16	0.16	0.16	0.16	0.14
Abs.corr.		0.24	0.29	0.23	0.20	0.11	0.23	0.25	0.24
Rel. corr.		0.49	0.54	0.48	0.49	0.46	0.55	0.52	0.51
sea ice freeboard [m]									
OIB bias	-0.11	0.01	-0.01	0.00	0.00	-0.07	-0.11	-0.10	-0.01
RMSE	0.12	0.07	0.07	0.07	0.07	0.09	0.12	0.12	0.06
Correlation	0.72	0.84	0.83	0.84	0.84	0.75	0.72	0.72	0.79
sea ice thickness [m]									
IceBird bias	-1.50	-0.66	-0.95	-0.88	-0.92	-1.14	-1.06	-1.02	-0.93
RMSE	1.86	1.20	1.30	1.24	1.33	1.53	1.49	1.49	1.34
Correlation	0.09	0.36	0.44	0.49	0.41	0.34	0.22	0.22	0.36
Mosaic bias	-1.31	0.39	-0.03	0.39	0.39	-0.12	-0.39	-0.57	-0.31
RMSE	1.33	0.49	0.22	0.50	0.50	0.40	0.65	0.80	0.47
Correlation	0.78	0.92	0.90	0.92	0.92	0.78	0.54	0.49	0.71
sea ice draft [m]									
BGEP bias	-0.73	0.10	-0.13	-0.07	-0.07	-0.29	-0.29	-0.32	-0.23
RMSE	0.87	0.41	0.33	0.33	0.33	0.46	0.45	0.49	0.41
Correlation	0.72	0.80	0.87	0.85	0.85	0.82	0.83	0.80	0.85
Laptev bias	-0.60	0.31	-0.15	-0.14	-0.14	-0.21	-0.23	-0.27	0.00
RMSE	0.80	0.61	0.50	0.51	0.51	0.52	0.49	0.52	0.48
Correlation	0.28	0.49	0.47	0.46	0.46	0.48	0.60	0.59	0.50
Barents bias	-0.38	0.27	-0.08	-0.02	0.18	-0.09	-0.11	-0.12	0.07
RMSE	0.51	0.70	0.54	0.52	0.43	0.33	0.35	0.36	0.38
Correlation	0.42	0.32	0.41	0.48	0.32	0.53	0.60	0.57	0.25

Table 2. Comparison of the various snow depth products against validation data of snow depth, sea ice freeboard, sea ice thickness and sea ice draft. Green colours indicate the best and red colours indicate the worst results (different scales for different quantities). For the buoys we calculate the correlation both for the absolute snow depth measurements (abs. corr.) and for the relative evolution since deployment (rel. corr.)

5.4 Validation of sea ice draft against moorings

While airborne data cover larger areas, moorings allow for a validation of the seasonal evolution. Furthermore, they complement the airborne analysis as most of the airborne data is over MYI, while the mooring data used here is mainly from FYI areas and the marginal ice zone. The longest record is available for the BGEP moorings (n=929). Here, we find generally very good correlation of 0.80-0.87 depending on the snow product vs. 0.72 assuming no snow. This again confirms that using any of the tested snow depth estimates adds skill versus assuming no snow -even when we only consider the summer data (see Figure 8). While mW99-IA yields the highest correlation, mW99-IC and mW99+SMLG (same in this area) perform best in terms of bias (-7 cm) and all three share the same lowest RMSE (33 cm). This is also confirmed visually (Figure 8), where SMLG, KuLa Clim and no snow often underestimate the snow and hence draft. However, all products capture the timing of the melt onset pretty well overall. In some years they match the mooring observations exactly, while in others they decline slightly too early. This might also be due to the large-scale averaging and errors in freeboard, ice density or snow density, which are the same for all snow depth products.

For the Laptev Sea moorings (n=218), KuLa Clim yields no bias and the lowest RMSE of 0.48 m. The highest correlation is achieved when using SMLG-M2 (0.60). Again, we observe a clear improvement when any of the snow products is used

https://doi.org/10.5194/egusphere-2026-5997
Preprint. Discussion started: 20 October 2026
© Author(s) 2026. CC BY 4.0 License.

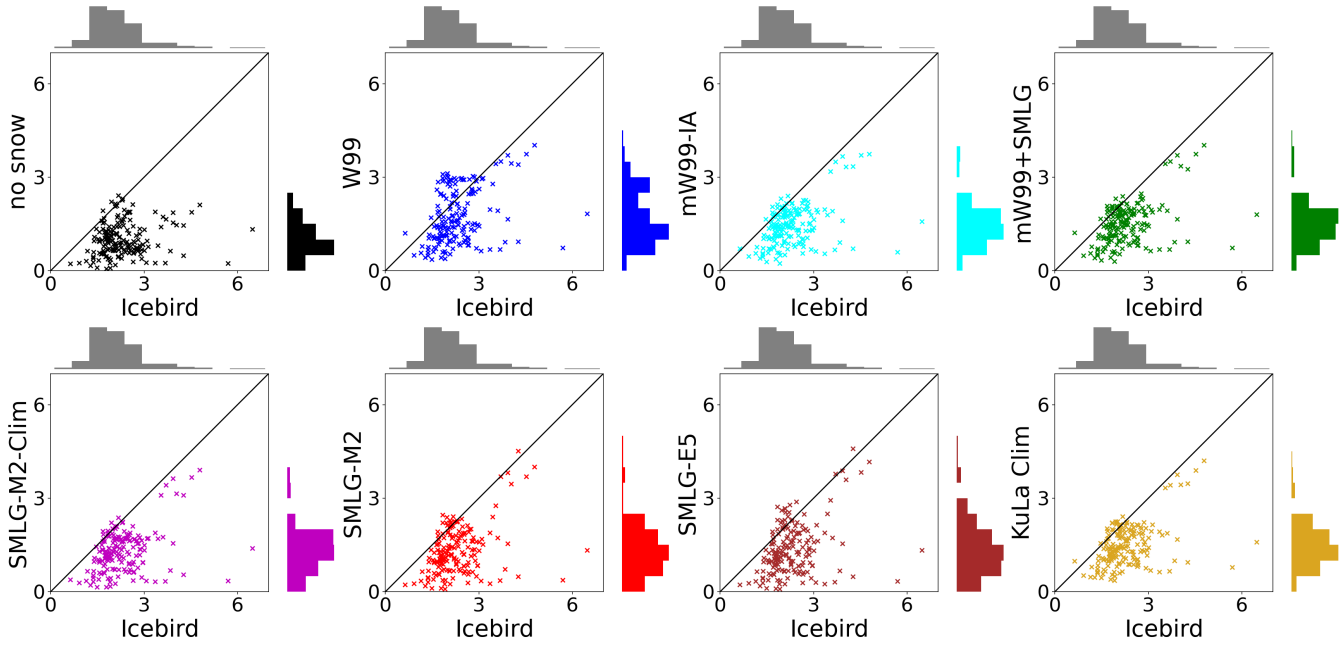


Figure 7. Sea ice thickness measured by IceBird [m] against CryoSat-2 based estimates using either no snow (first panel) or the various snow depth products where all snow products are valid. mW99-IC equals mW99+SMLG in the area where all products are valid (i.e. Central Arctic), so only the latter is shown.

compared to no snow. The modified Warren products yield lower biases, while the SMLG products yield higher correlations. The KuLa climatology stands out with a much lower bias than any other product, while the correlation is average (0.50).

The Barents Sea moorings are located at the edge of the well-defined Warren area. Hence, we only have 95 data points for (modified) Warren and 416 for the others. Where valid, mW99-IC yields the lowest bias (-0.02 m). The KuLa climatology has the lowest bias out of the products covering all mooring locations (0.07 m). In contrast, the SMLG-M2 Climatology gives the lowest RMSE of 0.33 m. Again, SMLG-M2 achieves the highest correlation of 0.60. Similar to the Laptev Sea moorings, different snow depth products perform best for different metrics. W99 clearly overestimates snow depth in these areas, but the modified Warren products yield decent biases where valid. On the other hand, the SMLG products yield lower RMSEs and higher correlations. The KuLa Clim also yields a low bias and RMSE, but also low correlation.

Overall, the mooring comparisons highlight various strength and weaknesses of the individual products. When the whole annual cycle is considered over multiple years, we find higher correlations from products that capture inter-annual anomalies, i.e. SMLG-M2 consistently outperforms the corresponding climatology in terms of correlation, but not in terms of bias and RMSE. Comparing the different forcing data (SMLG-M2 and SMLG-E5), we find that SMLG-M2 gives better results across all mooring datasets. For the buoy and airborne data, SMLG-M2 was also significantly better amongst the MOSAIC dataset and more or less the same for all others. Together with the observation that SMLG-E5 melts the snow much earlier than all other datasets, we therefore discourage using this version during the summer period. We also find that W99 overestimates snow

https://doi.org/10.5194/egusphere-2026-5997
Preprint. Discussion started: 20 October 2026
© Author(s) 2026. CC BY 4.0 License.

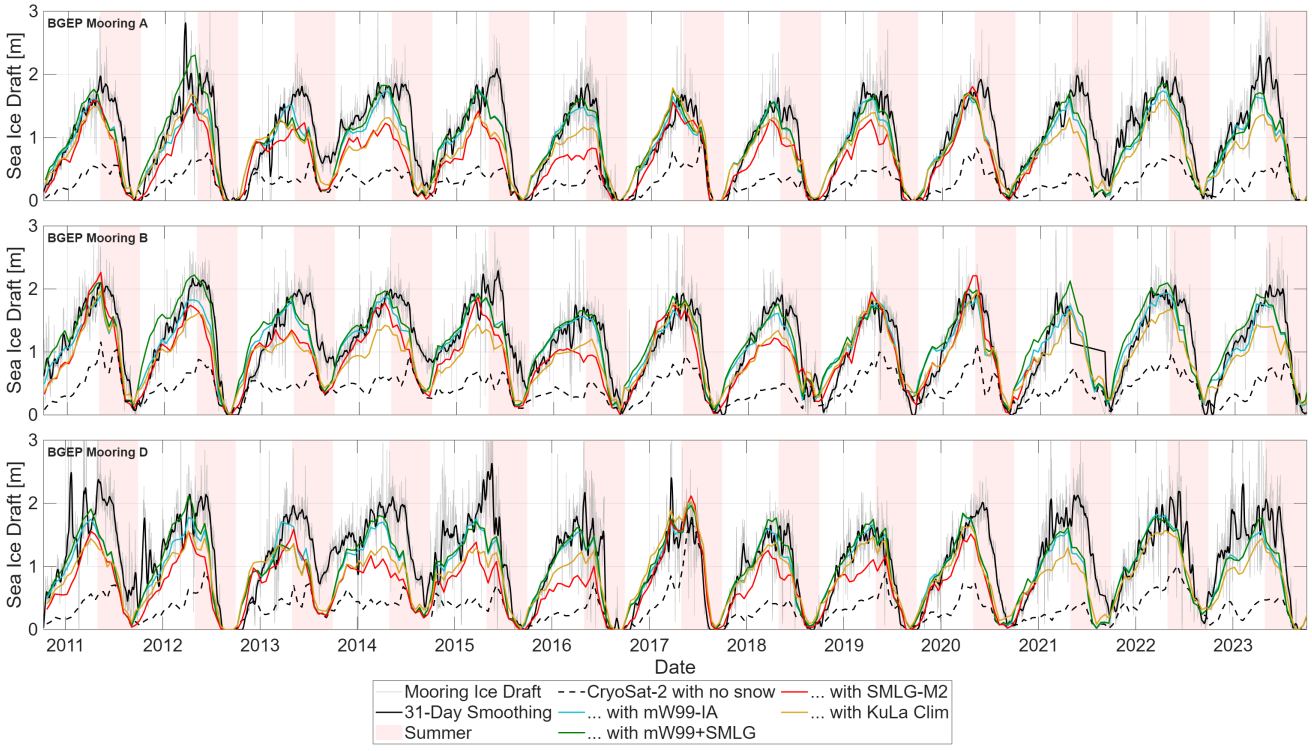


Figure 8. Temporal evolution of sea ice draft as measured by the BGEP moorings (grey for daily measurements and black for the rolling average) compared to sea ice draft estimated from CryoSat-2 freeboard assuming no snow (black dashed line) or using different snow depth estimates (coloured lines). The summer periods (May-September) are highlighted by red background shading.

in all mooring areas, which are dominated by FYI. The modified Warren products perform much better than W99. The KuLa climatology is a decent choice across most mooring metrics (except the correlation with the Barents Sea moorings).

5.5 Applicability of KuLa year-round

Overall, the intercomparison of the various year-round snow depth products and their validation against in situ data, suggests that KuLa dual-frequency altimetry is applicable year-round. The KuLa climatology often yields estimates that lie between the Warren based and SMLG based products. The biggest difference is the higher snow depth north of Greenland and the Canadian Arctic Archipelago and the higher remaining snow in August (Figures 2 and 3). This indicates that either the CryoSat-2 freeboards are biased low in summer or that the ICESat-2 ATL20 freeboards are biased high in summer - or both. This result is not unexpected. The raw radar freeboards from CryoSat-2 are known to be biased thin in mid-summer (Landy et al., 2022), although we attempt to mitigate this with the applied bias correction. New methods for processing the ICESat-2 data also lead to 1-5 cm thinner pan-Arctic freeboards than ATL20 (Liu et al., 2026). The maps (Figure 2) reveal that KuLa mainly yields thicker snow compared to the observation-based climatology from Warren close to the North coast of Greenland and

https://doi.org/10.5194/egusphere-2026-5997
Preprint. Discussion started: 20 October 2026
© Author(s) 2026. CC BY 4.0 License.

the Canadian Arctic Archipelago. For this region, particularly large differences between CryoSat-2 and ICESat-2 freeboard and SIT have been found year-round (Petty et al., 2025a; Carret et al., 2025; Zhou et al., 2021). This area is known to be especially ridged (Duncan and Farrell, 2022), so the fundamentally different footprint sizes of the two sensors will give very different height distributions and it is likely that the mean of ICESat-2 observations exceeds the mean from the lower resolution CryoSat-2 observations by some margin. If this is the reason, it would affect KuLa snow depth year-round and imply that KuLa snow depth estimates are also biased high in winter. A future experiment over snow free (i.e. fully melted) areas could be used to reveal biases between the two sensors, but would require ground truth data to identify such areas.

6 Conclusions

This study presented the first year-round assessment of different snow depth products derived from the Warren climatology, SnowModel-LG (SMLG), their combination (mW99+SMLG) and a first test of dual-altimetry snow (KuLa) year-round. Our comparisons show that using any of these snow depth products is better than assuming no snow. Even for mid/end July, the comparison to OIB data and direct observations used for the W99 climatology suggest that some snow is remaining at this time.

None of the snow depth products clearly outperformed the others amongst all comparisons. However, we discourage extrapolating the (modified) Warren climatology to areas outside of the Central Arctic, where it was defined, as unrealistic or even negative values occur e.g. in the Kara Sea, Barents Sea, Fram Strait and Baffin Bay. Our analysis also confirms that the original Warren climatology overestimates snow depth in the current Arctic. Nonetheless, the modified versions still perform well. The clearest difference between using the ice age product and ice charts to reduce snow depth over FYI areas was observed against the MOSAIC data. Here, and compared to the buoys, the ice age data gave better results. For SMLG, we found clear differences between the two versions. The MERRA-2 forced version yields a more realistic timing of snow ablation and performed better against validation data than the ERA-5 forced version, which melts the snow much faster than any other product. SMLG-M2 yields higher correlations than the corresponding climatology, when the temporal component is analysed, but actually performs worse for spatial patterns, implying that some of the local variability in snow depth is exaggerated. Finally, the KuLa dual-altimetry snow depth climatology was found to yield realistic results also in summer, mostly agreeing with the other products and validation data. However, compared to the other products, it kept higher snow depth in August, which indicates remaining negative biases in the CryoSat-2 and/or positive biases in the ICESat-2 data. Nevertheless, the initial assessment of a year-round application of KuLa is promising and these estimates are expected to improve as the work on CryoSat-2 and ICESat-2 summer classification and freeboard computation evolves.

For future work, we recommend further optimisation of ICESat-2, CryoSat-2 and future CRISTAL freeboard retrieval for the summer months, which would benefit the resulting KuLa estimates. At the moment the freeboard data is more noisy and sparse in summer, so only the climatology gives gap free, smooth maps. If more data becomes available from improved classification and summer processing techniques, KuLa could also be tested for individual years. And finally, if the latency of the ICESat-2 data could be reduced, KuLa could also become an option for operational processing. To date, NASA offers a quicklook version

https://doi.org/10.5194/egusphere-2026-5997
Preprint. Discussion started: 20 October 2026
© Author(s) 2026. CC BY 4.0 License.

of ATL10 along-track freeboards with a latency of 3 days, while the latency of the higher quality ATL10 and gridded ATL20 data is around 2 and 6 months respectively. The lack of operational production also limits the use of SMLG data for many applications. Here, using climatologies (together with MYI concentration data from ice charts if W99 is used) is currently the only option.

Furthermore, data assimilation and many other tasks require uncertainty information, but most snow depth estimates do not come with uncertainty estimates. Indeed, the only uncertainty estimates available from the year-round snow depth products are derived from snow depth variability within the climatology time periods. Therefore, we also recommend deriving reliable uncertainty estimates. The validation and intercomparison exercises from this study give a first indication for what is realistic: The products disagree most in June and agree best in August. As a whole, the summer months yield the same variability amongst the different estimates than for the winter months (4 cm each) and there is no obvious difference in the agreement against buoy observations between summer and winter as a whole. However, the period around melt onset (June) appears to be the most uncertain. To really quantify the uncertainties, more in-situ timeseries of the snow depth distribution are needed and to date these are limited to individual point measurements. The deployment of many buoys around the same area - as done during MOSAIC - can compensate some of the representation issue and should be repeated in future years and different areas. Also, continuous deployments on young ice may be necessary so that available buoy data does not only cover the oldest sea ice classes at the transition from winter to summer. This will also be essential to investigate CRISTAL measurements of snow depth year-round. When SIT is compared, many other uncertainties mask the impact of snow depth, so it is hard to determine the actual snow depth uncertainty or to identify the most accurate snow depth estimate. On the other hand, testing the impact on SIT revealed clear differences between the products and we found that the combination of CryoSat-2 freeboard and either a modified Warren climatology or the KuLa climatology yielded better results over rougher MYI, while we found mixed results over FYI.

Data availability. All input data used to perform this assessment is freely available (see Data section for the respective dois).

Appendix A: Evolution of snow depth since buoy deployment

Author contributions. ABF, JL and ADB designed the study. SH developed the mW99+SMLG snow depth. JL developed the method and code to convert radar freeboard to SIT and to validate against airborne and mooring data. CV performed early work on the validation of SMLG in summer, supervised by ABF. ABF developed all other methods and code, performed the analysis and created the figures. ABF, JL, RR and ADB discussed the interpretation. ABF wrote the initial draft of the paper. All authors contributed to review and editing.

Competing interests. The authors have no competing interests.

https://doi.org/10.5194/egusphere-2026-5997
Preprint. Discussion started: 20 October 2026
© Author(s) 2026. CC BY 4.0 License.

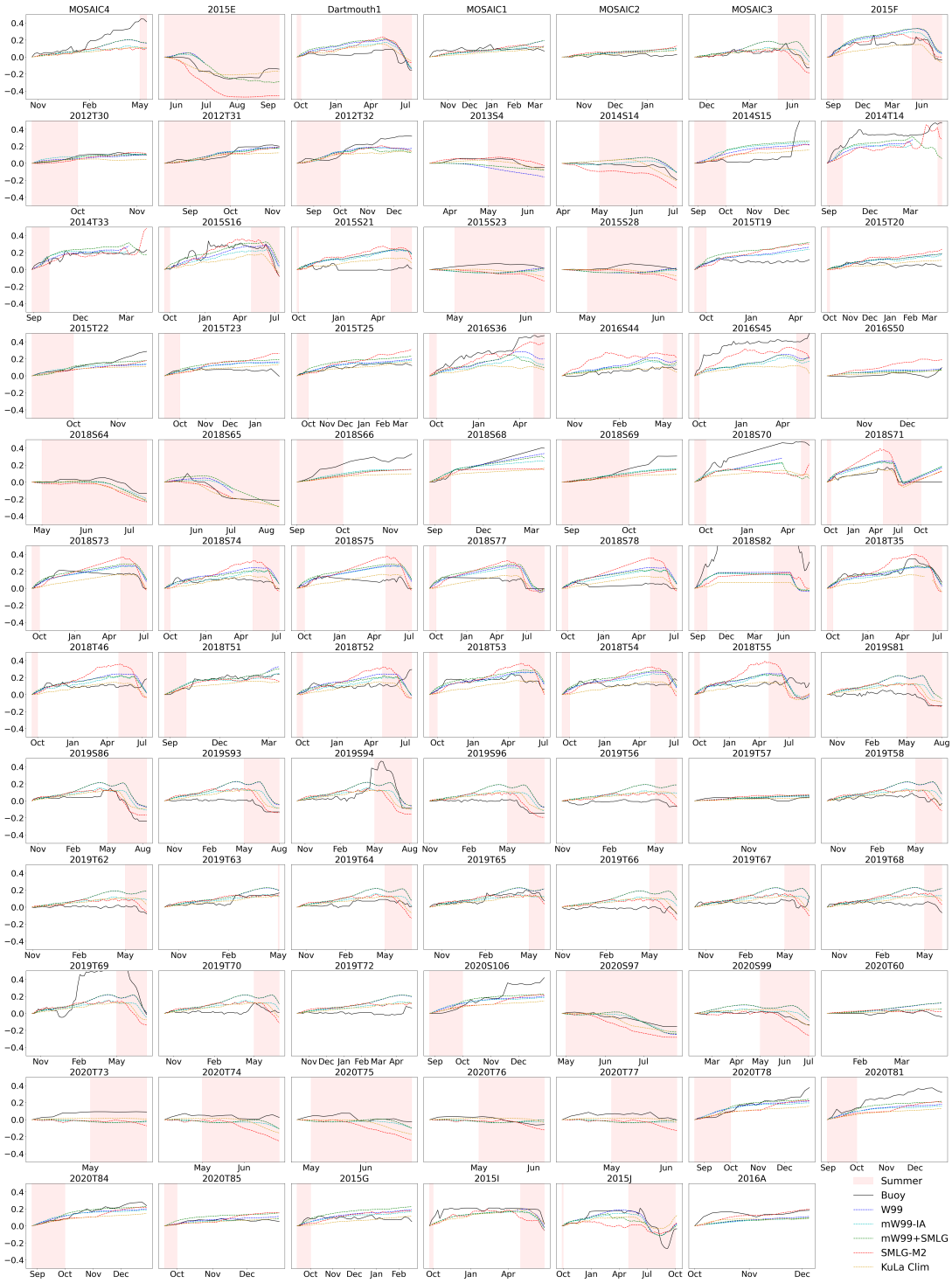


Figure A1. Evolution of snow depth since buoy deployment (first point set to zero) as measured in situ (black) and estimated by the various snow depth products (colour). The summer season (May-September) is highlighted by red shading. Please note that all plots share the same y-axis of relative snow depth evolution [m], but the time periods over which each buoy recorded data (x-axes) vary significantly.

https://doi.org/10.5194/egusphere-2026-5997
Preprint. Discussion started: 20 October 2026
© Author(s) 2026. CC BY 4.0 License.



Acknowledgements. This work was funded by ESA through the CryoTEMPO project (Contract AO/1-10244/2-/I-NS). ABF, JL and RR also received funding by ESA's CLEV2ER project (Contract AO/1-11448/22/I-AG) and ABF and JL received funding through NFR grant 363568 Arctic Ocean 2050. The CryoSat-2 sea-ice thickness processor development was funded through the ERC Starting Grant SI/3D (101077496). ChatGPT v5 was used to generate code snippets and for debugging.

https://doi.org/10.5194/egusphere-2026-5997
Preprint. Discussion started: 20 October 2026
© Author(s) 2026. CC BY 4.0 License.

References

Belter, H., Krumpen, T., Albedyll, L., Alekseeva, T., Birnbaum, G., Frolov, S., and Ricker, R.: Interannual variability in Transpolar Drift summer sea ice thickness and potential impact of Atlantification, Cryosphere, 15, 2575–2591, https://doi.org/10.5194/tc-15-2575-2021, 2021.

Belter, H. J., Janout, M. A., Krumpen, T., Ross, E., Hölemann, J. A., Timokhov, L., Novikhin, A., Kassens, H., Wyatt, G., Rousseau, S., and Sadowy, D.: Daily mean sea ice draft from moored Upward-Looking Sonars in the Laptev Sea between 2013 and 2015, https://doi.org/10.1594/PANGAEA.899275, 2019.

Belter, H. J., Janout, M. A., Hölemann, J. A., and Krumpen, T.: Daily mean sea ice draft from moored upward-looking Acoustic Doppler Current Profilers (ADCPs) in the Laptev Sea from 2003 to 2016, https://doi.org/10.1594/PANGAEA.912927, 2020.

Braakmann-Folgmann, A. and Donlon, C.: Estimating snow depth on Arctic sea ice using satellite microwave radiometry and a neural network, Cryosphere, 13, 2421–2438, https://doi.org/10.5194/tc-13-2421-2019, 2019.

Braakmann-Folgmann, A., Landy, J. C., Dawson, G., and Ricker, R.: Enhanced neural network classification for Arctic summer sea ice, Cryosphere, 20, 905–929, https://doi.org/10.5194/tc-20-905-2026, 2026.

Buckley, E. M., Kacimi, S., Webster, M., Harrison, S., Saylam, K., Kurtz, N. T., and Tilling, R. L.: First Assessment of ICESat-2 Summer Sea Ice Freeboard With Airborne Validation, Geophysical Research Letters, 53, https://doi.org/10.1029/2026GL124704, 2026.

Carret, A., Fleury, S., Di Bella, A., Landy, J., Lawrence, I., Kurtz, N., Laforge, A., Bouffard, J., and Parrinello, T.: A multi-frequency altimetry snow depth product over Arctic sea ice, Scientific Data, 12, https://doi.org/10.1038/s41597-024-04343-4, 2025.

Chapman-Dutton, H. R. and Webster, M. A.: The Effects of Summer Snowfall on Arctic Sea Ice Radiative Forcing, Journal of Geophysical Research: Atmospheres, 129, https://doi.org/10.1029/2023JD040667, 2024.

Comiso, J. C., Cavalieri, D. J., and Markus, T.: Sea ice concentration, ice temperature, and snow depth using AMSR-E data, IEEE Transactions on Geoscience and Remote Sensing, 41, 243–252, https://doi.org/10.1109/TGRS.2002.808317, 2003.

Dawson, G., Landy, J., Tsamados, M., Komarov, A. S., Howell, S., Heorton, H., and Krumpen, T.: A 10-year record of Arctic summer sea ice freeboard from CryoSat-2, Remote Sensing of Environment, 268, https://doi.org/10.1016/j.rse.2021.112744, 2022.

Divine, D. V., Steer, A., Granskog, M. A., Gerland, S., Foss, , Cristea, A., Itkin, P., Johansson, M., Down, E., and Fransson, A.: Data on Physical Properties of Sea Ice in the Northern Barents Sea and Adjacent Arctic Basin From the Nansen Legacy Project, Geoscience Data Journal, 12, e70 001, https://doi.org/https://doi.org/10.1002/gdj3.70001, e70001 GDJ-2024-11-0078.R1, 2025.

Duncan, K. and Farrell, S. L.: Determining Variability in Arctic Sea Ice Pressure Ridge Topography With ICESat-2, Geophysical Research Letters, 49, https://doi.org/10.1029/2022GL100272, 2022.

European Space Agency: Cryo-TEMPO Sea Ice Thematic Product (TEMPO_SILI-PO_SI), Distributed by UCL/CPOM and ESA Earth Online, https://doi.org/10.5270/CR2-e2dd631, accessed: 2026-09-29, 2026.

Guerreiro, K., Fleury, S., Zakharova, E., Rémy, F., and Kouraev, A.: Potential for estimation of snow depth on Arctic sea ice from CryoSat-2 and SARAL/AltiKa missions, Remote Sensing of Environment, 186, 339–349, https://doi.org/10.1016/j.rse.2016.07.013, 2016.

Hamilton, C. D., Kovacs, K. M., Ims, R. A., Aars, J., and Lydersen, C.: An Arctic predator–prey system in flux: climate change impacts on coastal space use by polar bears and ringed seals, Journal of Animal Ecology, 86, 1054–1064, 2017.

Hendricks, S.: Monthly Arctic Snow on Sea Ice Climatology Combining SnowModel-LG and Warren99 (Version 1.1), https://doi.org/10.5281/zenodo.22675171, 2026.

https://doi.org/10.5194/egusphere-2026-5997
Preprint. Discussion started: 20 October 2026
© Author(s) 2026. CC BY 4.0 License.

Itkin, P., Hendricks, S., Webster, M., von Albedyll, L., Arndt, S., Divine, D., Jaggi, M., Oggier, M., Raphael, I., Ricker, R., Rohde, J., Schneebeli, M., and Liston, G. E.: Sea ice and snow characteristics from year-long transects at the MOSAiC Central Observatory, Elementa, 11, https://doi.org/10.1525/elementa.2022.00048, 2023.

Jutila, A., Hendricks, S., Ricker, R., von Albedyll, L., and Haas, C.: Airborne sea ice parameters during the IceBird Winter 2019 campaign in the Arctic Ocean, Version 2, 2024.

Kacimi, S. and Kwok, R.: Arctic Snow Depth, Ice Thickness, and Volume From ICESat-2 and CryoSat-2: 2018–2021, Geophysical Research Letters, 49, https://doi.org/10.1029/2021GL097448, 2022.

Kauko, H. M., Taskjelle, T., Assmy, P., Pavlov, A. K., Mundy, C. J., Duarte, P., Fernández-Méndez, M., Olsen, L. M., Hudson, S. R., Johnsen, G., Elliott, A., Wang, F., and Granskog, M. A.: Windows in Arctic sea ice: Light transmission and ice algae in a refrozen lead, Journal of Geophysical Research: Biogeosciences, 122, 1486–1505, https://doi.org/10.1002/2016JG003626, 2017.

Krumpen, T., von Albedyll, L., Bünger, H. J., Castellani, G., Hartmann, J., Helm, V., Hendricks, S., Hutter, N., Landy, J. C., Lisovski, S., et al.: Smoother sea ice with fewer pressure ridges in a more dynamic Arctic, Nature Climate Change, 15, 66–72, 2025.

Kurtz, N. T. and Farrell, S. L.: Large-scale surveys of snow depth on Arctic sea ice from Operation IceBridge, Geophysical Research Letters, 38, https://doi.org/10.1029/2011GL049216, 2011.

Landy, J., Braakmann-Folgmann, A., Salganik, E., Glissenaar, I., Lechler, L., and Chenal, A.: An Updated Year-Round CryoSat-2 Sea Ice Thickness Dataset for the Arctic Ocean: 2010-2024, 2026a.

Landy, J. C., Petty, A. A., Tsamados, M., and Stroeve, J. C.: Sea Ice Roughness Overlooked as a Key Source of Uncertainty in CryoSat-2 Ice Freeboard Retrievals, Journal of Geophysical Research: Oceans, 125, https://doi.org/10.1029/2019JC015820, 2020.

Landy, J. C., Dawson, G. J., Tsamados, M., Bushuk, M., Stroeve, J. C., Howell, S. E., Krumpen, T., Babb, D. G., Komarov, A. S., Heorton, H. D., Belter, H. J., and Aksenov, Y.: A year-round satellite sea-ice thickness record from CryoSat-2, Nature, 609, 517–522, https://doi.org/10.1038/s41586-022-05058-5, 2022.

Landy, J. C., de Rijke-Thomas, C., Nab, C., Lawrence, I., Glissenaar, I. A., Mallett, R. D. C., Fredensborg Hansen, R. M., Petty, A., Tsamados, M., Macfarlane, A. R., and Braakmann-Folgmann, A.: Anticipating CRISTAL: an exploration of multi-frequency satellite altimeter snow depth estimates over Arctic sea ice, 2018–2023, The Cryosphere, 20, 183–208, https://doi.org/10.5194/tc-20-183-2026, 2026b.

Lavergne, T., Macdonald Sørensen, A., Kern, S., Tonboe, R., Notz, D., Aaboe, S., Bell, L., Dybkjær, G., Eastwood, S., Gabarro, C., Heygster, G., Anne Killie, M., Brandt Kreiner, M., Lavelle, J., Saldo, R., Sandven, S., and Pedersen, L. T.: Version 2 of the EUMETSAT OSI SAF and ESA CCI sea-ice concentration climate data records, Cryosphere, 13, 49–78, https://doi.org/10.5194/tc-13-49-2019, 2019.

Lawrence, I., Tsamados, M., Stroeve, J., Armitage, T., and Ridout, A.: Estimating snow depth over Arctic sea ice from calibrated dual-frequency radar freeboards, https://doi.org/10.5194/tc-2018-54, 2018.

Lei, R., Cheng, B., Hoppmann, M., and Zuo, G.: Snow depth and sea ice thickness derived from the measurements of SIMBA buoys deployed in the Arctic Ocean during the Legs 1a, 1, and 3 of the MOSAiC campaign in 2019-2020, https://doi.org/10.1594/PANGAEA.938244, 2021.

Liston, G., Stroeve, J., and Itkin, P.: Lagrangian Snow Distributions for Sea-Ice Applications, Version 1, https://doi.org/10.5067/27A0P5M6LZBI, 2021.

Liston, G. E., Itkin, P., Stroeve, J., Tschudi, M., Stewart, J. S., Pedersen, S. H., Reinking, A. K., and Elder, K.: A Lagrangian Snow-Evolution System for Sea-Ice Applications (SnowModel-LG): Part I—Model Description, Journal of Geophysical Research: Oceans, 125, https://doi.org/10.1029/2019JC015913, 2020.

https://doi.org/10.5194/egusphere-2026-5997
Preprint. Discussion started: 20 October 2026
© Author(s) 2026. CC BY 4.0 License.

Liu, W., Lei, R., Jin, T., Sun, H., Tsamados, M., Glissenaar, I. A., Landy, J. C., and Zhou, Y.: Year-Round High-Resolution Sea Ice Freeboard Retrieval Using ICESat-2 ATL03 Photon Data, The Cryosphere, 20, 4839–4876, https://doi.org/10.5194/tc-20-4839-2026, 2026.

Mallett, R. D.: A methodologically robust densification function for snow on multiyear Arctic sea ice, Journal of Glaciology, 71, https://doi.org/10.1017/jog.2025.5, 2025.

Markus, T., Powell, D. C., and Wang, J. R.: Sensitivity of passive microwave snow depth retrievals to weather effects and snow evolution, IEEE Transactions on Geoscience and Remote Sensing, 44, 68–77, https://doi.org/10.1109/TGRS.2005.860208, 2006.

Markus, T., Stroeve, J. C., and Miller, J.: Recent changes in Arctic sea ice melt onset, freezeup, and melt season length, Journal of Geophysical Research: Oceans, 114, https://doi.org/10.1029/2009JC005436, 2009.

Nicolaus, M., Hoppmann, M., Arndt, S., Hendricks, S., Katlein, C., König-Langlo, G., Nicolaus, A., Rossmann, L., Schiller, M., Schwegmann, S., Langevin, D., and Bartsch, A.: Snow height and air temperature on sea ice from Snow Buoy measurements [dataset], 2017.

Nicolaus, M., Perovich, D. K., Spreen, G., Granskog, M. A., von Albedyll, L., Angelopoulos, M., Anhaus, P., Arndt, S., Jakob Belter, H., Bessonov, V., Birnbaum, G., Brauchle, J., Calmer, R., Cardellach, E., Cheng, B., Clemens-Sewall, D., Dadic, R., Damm, E., de Boer, G., Demir, O., Dethloff, K., Divine, D. V., Fong, A. A., Fons, S., Frey, M. M., Fuchs, N., Gabarró, C., Gerland, S., Goessling, H. F., Gradinger, R., Haapala, J., Haas, C., Hamilton, J., Hannula, H. R., Hendricks, S., Herber, A., Heuzé, C., Hoppmann, M., Høyland, K. V., Huntemann, M., Hutchings, J. K., Hwang, B., Itkin, P., Jacobi, H. W., Jaggi, M., Jutila, A., Kaleschke, L., Katlein, C., Kolabutin, N., Krampe, D., Kristensen, S. S., Krumpen, T., Kurtz, N., Lampert, A., Lange, B. A., Lei, R., Light, B., Linhardt, F., Liston, G. E., Loose, B., Macfarlane, A. R., Mahmud, M., Matero, I. O., Maus, S., Morgenstern, A., Naderpour, R., Nandan, V., Niubom, A., Oggier, M., Oppelt, N., Pätzold, F., Perron, C., Petrovsky, T., Pirazzini, R., Polashenski, C., Rabe, B., Raphael, I. A., Regnery, J., Rex, M., Ricker, R., Riemann-Campe, K., Rinke, A., Rohde, J., Salganik, E., Scharien, R. K., Schiller, M., Schneebeli, M., Semmling, M., Shimanchuk, E., Shupe, M. D., Smith, M. M., Smolyanitsky, V., Sokolov, V., Stanton, T., Stroeve, J., Thielke, L., Timofeeva, A., Tonboe, R. T., Tavri, A., Tsamados, M., Wagner, D. N., Watkins, D., Webster, M., and Wendisch, M.: Overview of the MOSAiC expedition: Snow and sea ice, Elementa, 10, https://doi.org/10.1525/elementa.2021.000046, 2022.

Onarheim, I. H., Årthun, M., Teigen, S. H., Eik, K. J., and Steele, M.: Recent Thickening of the Barents Sea Ice Cover, Geophysical Research Letters, 51, https://doi.org/10.1029/2024GL108225, 2024.

Petty, A., Cabaj, A., and Landy, J. C.: Initial assessment of all-season Arctic sea ice thickness from ICESat-2, Journal of Glaciology, 72, https://doi.org/10.1017/jog.2025.10119, 2025a.

Petty, A., Kwok, R., Bagnardi, M., Ivanoff, A., Kurtz, N., Lee, J., Wimert, J., and Hancock, D.: ATLAS/ICESat-2 L3B Daily and Monthly Gridded Sea Ice Freeboard, Version 5, https://doi.org/10.5067/ATLAS/ATL20.005, 2025b.

Preußer, A., Nicolaus, M., and Hoppmann, M.: Snow depth, sea ice thickness and interface temperatures derived from measurements of SIMBA buoy 2016T37, https://doi.org/10.1594/PANGAEA.973396, in: Preußer, A et al. (2025): Snow depth, sea ice thickness and interface temperatures derived from measurements of SIMBA buoys deployed in the Arctic Ocean and Southern Ocean between 2012 and 2023 [dataset publication series]. PANGAEA, https://doi.org/10.1594/PANGAEA.973193, 2025.

Ricker, R., Hendricks, S., Helm, V., Skourup, H., and Davidson, M.: Sensitivity of CryoSat-2 Arctic sea-ice freeboard and thickness on radar-waveform interpretation, Cryosphere, 8, 1607–1622, https://doi.org/10.5194/tc-8-1607-2014, 2014.

Rostosky, P., Spreen, G., Farrell, S. L., Frost, T., Heygster, G., and Melsheimer, C.: Snow Depth Retrieval on Arctic Sea Ice From Passive Microwave Radiometers—Improvements and Extensions to Multiyear Ice Using Lower Frequencies, Journal of Geophysical Research: Oceans, 123, 7120–7138, https://doi.org/10.1029/2018JC014028, 2018.

https://doi.org/10.5194/egusphere-2026-5997
Preprint. Discussion started: 20 October 2026
© Author(s) 2026. CC BY 4.0 License.

Salganik, E. and Landy, J.: Snow and sea ice thickness derived from measurements of CRREL ice mass balance buoys between 1997 and 2024, https://doi.org/10.5281/zenodo.15096485, 2025.

Shalina, E. V. and Sandven, S.: Snow depth on Arctic sea ice from historical in situ data, Cryosphere, 12, 1867–1886, https://doi.org/10.5194/tc-12-1867-2018, 2018.

Sievers, I., Skourup, H., and Rasmussen, T. A.: Impact assessment of snow thickness, sea ice density and water density in CryoSat-2-derived sea ice thickness, Cryosphere, 18, 5985–6004, https://doi.org/10.5194/tc-18-5985-2024, 2024.

Song, R., Mu, L., Loza, S. N., Kauker, F., and Chen, X.: Assimilating summer sea-ice thickness observations improves Arctic sea-ice forecast, Geophysical Research Letters, 51, e2024GL110 405, 2024.

Steele, M., Bliss, A., Peng, G., Meier, W., and Dickinson, S.: Arctic Sea Ice Seasonal Change and Melt/Freeze Climate Indicators from Satellite Data, Version 2, https://doi.org/10.5067/2ZJKKYXYLYZ0, 2026.

Stroeve, J., Liston, G. E., Buzzard, S., Zhou, L., Mallett, R., Barrett, A., Tschudi, M., Tsamados, M., Itkin, P., and Stewart, J. S.: A Lagrangian Snow Evolution System for Sea Ice Applications (SnowModel-LG): Part II—Analyses, Journal of Geophysical Research: Oceans, 125, https://doi.org/10.1029/2019JC015900, 2020.

Sturm, M., Holmgren, J., and Perovich, D. K.: Winter snow cover on the sea ice of the Arctic Ocean at the Surface Heat Budget of the Arctic Ocean (SHEBA): Temporal evolution and spatial variability, Journal of Geophysical Research: Oceans, 107, https://doi.org/10.1029/2000jc000400, 2002.

Taelman, C., Landy, J., Mallett, R., and Itkin, P.: Empirical evidence of overestimated Ku-band sea ice radar freeboards in satellite altimetry, https://doi.org/10.5194/egusphere-2026-1662, 2026.

Tschudi, M., Meier, W., and Stewart, J.: Quicklook Arctic Weekly EASE-Grid Sea Ice Age, Version 1, https://doi.org/10.5067/2XXGZY3DUGNQ, 2019a.

Tschudi, M., Meier, W., Stewart, J., Fowler, C., and Maslanik, J.: EASE-Grid Sea Ice Age, Version 4, https://doi.org/10.5067/UTAV7490FEPB, 2019b.

Ulaby, F. T. and Long, D. G.: Microwave radar and radiometric remote sensing, The University of Michigan Press, ISBN 9780472119356, 0472119354, 2014.

U.S. National Ice Center: U.S. National Ice Center Arctic and Antarctic Sea Ice Concentration and Climatologies in Gridded Format, https://doi.org/10.7265/46CC-3952, 2020.

von Albedyll, L., Haas, C., and Grodofzig, R.: EM-Bird ice thickness measurements in the Transpolar Drift during MOSAiC 2019/2020, part 1, https://doi.org/10.1594/PANGAEA.934578, 2021.

Warren, S. G., Rigor, I. G., Untersteiner, N., Radionov, V. F., Bryazgin, N. N., and Aleksandrov, Y. I.: Snow Depth on Arctic Sea Ice, Journal of Climate, 12, 1999.

Wever, N., Leonard, K., Maksym, T., White, S., Proksch, M., and Lenaerts, J. T.: Spatially distributed simulations of the effect of snow on mass balance and flooding of Antarctic sea ice, Journal of Glaciology, 67, 1055–1073, 2021.

Zhang, J. and Rothrock, D. A.: Modeling Global Sea Ice with a Thickness and Enthalpy Distribution Model in Generalized Curvilinear Coordinates, Monthly Weather Review, https://doi.org/10.1175/1520-0493(2003)131<0845:MGSIWA>2.0.CO;2, 2003.

Zhang, Y.-F., Bushuk, M., Winton, M., Hurlin, B., Gregory, W., Landy, J., and Jia, L.: Improvements in september arctic sea ice predictions via assimilation of summer CryoSat-2 sea ice thickness observations, Geophysical Research Letters, 50, e2023GL105 672, 2023.

https://doi.org/10.5194/egusphere-2026-5997
Preprint. Discussion started: 20 October 2026
© Author(s) 2026. CC BY 4.0 License.



Zhou, L., Stroeve, J., Xu, S., Petty, A., Tilling, R., Winstrup, M., Rostosky, P., Lawrence, I. R., Liston, G. E., Ridout, A., Tsamados, M., and Nandan, V.: Inter-comparison of snow depth over Arctic sea ice from reanalysis reconstructions and satellite retrieval, Cryosphere, 15, 345–367, https://doi.org/10.5194/tc-15-345-2021, 2021.

Zhuang, J., Dussin, R., Huard, D., Bourgault, P., Banihirwe, A., Raynaud, S., Malevich, B., Schupfner, M., Hamman, J., Levang, S., Jüling, A., Almansi, M., Fernandes, F., Rondeau-Genesse, G., Rasp, S., and Bell, R.: xESMF: v0.7.0, https://doi.org/10.5281/zenodo.7447707, 2022.

Zygmuntowska, M., Rampal, P., Ivanova, N., and Smedsrud, L. H.: Uncertainties in Arctic sea ice thickness and volume: New estimates and implications for trends, Cryosphere, 8, 705–720, https://doi.org/10.5194/tc-8-705-2014, 2014.